

The Use of a Water Mist Curtain as a Radiation Shield

Daniel A. Martin

**Department of Fire Safety Engineering
Lund University, Sweden**

Report 5497, Lund 2015



HOST UNIVERSITY: Lund University

FACULTY: Faculty of Engineering

DEPARTMENT: Department of Fire Safety Engineering

Academic Year 2014-2015

The Use of a Water Mist Curtain as a Radiation Shield

Daniel A. Martin

Promoter: Bjarne Husted

Master thesis submitted in the Erasmus Mundus Study Programme

International Master of Science in Fire Safety Engineering

Title: The Use of a Water Mist Curtain as a Radiation Shield

Author: Daniel A. Martin

Report 5497

ISRN: LUTVDG/TVBB—5497--SE

Number of pages: 78

Keywords:

Radiation attenuation, water mist, water curtain, radiation

Abstract

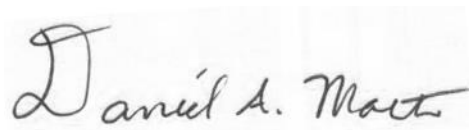
Water mist systems have seen an increase in use as an alternative clean agent fire suppressant since the late 1980's after the use of Halon gases were discontinued. One of the potential uses of these systems is to provide a protective curtain between a fire and desired target. The following experimental work investigates the radiation attenuation abilities of a single water mist spray. These experimental results are the first ever conducted with high pressure water mist. Two sources of heat flux were utilized: radiant panel and diffusion flame line burner. Radiation levels were measured along the normal propagation path and at an angle of $\pm 5^\circ$ above and below the normal in the vertical plane. Attenuation levels were found to be greater than 40% for all locations 300+ mm below the nozzle. Initially the attenuation is high near the nozzle, decreases in intensity until 200 mm, rises again until the 500 mm mark, and then experiences a slight decrease below 500 mm. This S-curve shaped attenuation distribution is attributed to the droplet size, volumetric water concentration, and residency time of the droplets. Water mist curtains can be an effective way of protecting high value targets from radiation.

© Copyright: Fire Safety Engineering, Lund University
Lund 2015.

Department of Fire Safety
Engineering
Lund University
P.O. Box 118
SE-221 00 Lund
Sweden
<http://www.brand.lth.se>
Telephone: +46 46 222 73 60

Disclaimer

“This thesis is submitted in partial fulfillment of the requirements for the degree of The International Master of Science in Fire Safety Engineering (IMFSE). This thesis has never been submitted for any degree or examination to any other University/program. The author(s) declare(s) that this thesis is original work except where stated. This declaration constitutes an assertion that full and accurate references and citations have been included for all material, directly included and indirectly contributing to the thesis. The author(s) gives (give) permission to make this master thesis available for consultation and to copy parts of this master thesis for personal use. In the case of any other use, the limitations of the copyright have to be respected, in particular with regard to the obligation to state expressly the source when quoting results from this master thesis. The thesis supervisor must be informed when data or results are used.”

A handwritten signature in black ink that reads "Daniel A. Martin". The signature is written in a cursive style with a large initial 'D'.

Daniel A. Martin

24 May 2015

“Read and Approved”

Abstract

Water mist systems have seen an increase in use as an alternative clean agent fire suppressant since the late 1980s after the use of Halon gases were discontinued. One of the potential uses of these systems is to provide a protective curtain between a fire and desired target. The following experimental work investigates the radiation attenuation abilities of a single water mist spray. These experimental results are the first ever conducted with high pressure water mist. Two sources of heat flux were utilized: radiant panel and diffusion flame line burner. Radiation levels were measured along the normal propagation path and at an angle of $\pm 5^\circ$ above and below the normal in the vertical plane. Attenuation levels were found to be greater than 40% for all locations 300+ mm below the nozzle. Initially the attenuation is high near the nozzle, decreases in intensity until 200 mm, rises again until the 500 mm mark, and then experiences a slight decrease below 500 mm. This S-curve shaped attenuation distribution is attributed to the droplet size, volumetric water concentration, and residency time of the droplets. Water mist curtains can be an effective way of protecting high value targets from radiation.

Table of Contents

Abstract.....	iii
Table of Contents.....	v
List of Symbols.....	vii
List of Tables.....	ix
List of Figures.....	xi
Foreword.....	xiii
1. Introduction.....	1
1.1 Objectives.....	2
1.2 Limitations.....	2
2. Literature Review.....	3
2.1 Water Mist Systems.....	3
2.2 Droplet Formation and Characterization.....	4
2.3 How Water Mist Systems Work.....	6
2.3.1 Theoretical Research.....	7
2.3.2 Experimental Research.....	8
3. Theoretical Calculation Approach for Radiation and Scattering.....	11
3.1 Radiation Calculation.....	11
3.2 Volumetric Water Concentration.....	15
3.3 Mie Scatter.....	15
4. Methodology.....	21
4.1 Water Mist Characteristics.....	22
4.2 Experimental Setup/Procedure.....	26
4.2.1 Equipment.....	26
4.2.2 Procedure.....	27
5. Results.....	31
5.1 Radiant Panel.....	31
5.2 Diffusion Flame Line Burner.....	32
5.3 Uncertainties in the Results.....	34
6. Discussion.....	37
6.1 Comparison between Theoretical and Experimental Baseline Radiation Levels.....	37

6.2 Radiant Panel	38
6.3 Diffusion Flame Line Burner	39
6.4 General Remarks	40
7. Conclusion	41
8. Future Work	43
9. Acknowledgements	45
10. References	47
Appendix A: Photographs	I
Appendix B: Flow Rate Test Procedure	III
Appendix C: Heat Flux Gauge Calibration	V
Appendix D: Experimental Procedure	VII
Appendix E: Risk Assessment	XV

List of Symbols

D_{10}	Length Based Mean Diameter (μm)
D_{20}	Surface Based Mean Diameter (μm)
D_{32}	Sauter Mean Diameter (μm)
D_{30} or D_v	Volume Based Mean Diameter (μm)
$D_v0.5$	50 percentile Volume Based Mean Diameter (μm)
F	View factor
T	Temperature (Kelvin)
\dot{Q}	Heat Release Rate (kW)
\dot{Q}''	Total Heat Flux (kW/m^2)
\dot{Q}''_{rad}	Radiative Heat Flux (kW/m^2)
ε	Emissivity
σ	Stefan-Boltzmann constant ($5.67 \times 10^{-5} \text{ kW}/\text{m}^2 \cdot \text{K}^4$)
χ	Radiative Fraction
L	Length of the flame from a line burner (m)
B	Longer dimension of the line burner (m)
i	Radiation Intensity
λ	Radiation Wavelength Size
S	Volume Size
K_a	Absorption Coefficient
K_s	Scattering Coefficient
i_b	Black Body Radiation Intensity
$\dot{Q}''_{rad,w/o mist(H_2O)}$	Radiative Heat Flux Without Water Mist Through the Spray (kW/m^2)
$\dot{Q}''_{total rad,w/o mist}$	Total Radiative Heat Flux Without Water Mist (kW/m^2)
$\dot{Q}''_{total rad,with mist}$	Total Radiative Heat Flux With Water Mist (kW/m^2)
$\dot{Q}''_{rad,w/o mist(unimpeded)}$	Unimpeded Radiative Heat Flux Without Water Mist (kW/m^2)
$\dot{Q}''_{rad,with mist(H_2O)}$	Radiative Heat Flux With Water Mist Through the Spray (kW/m^2)
a	Unimpeded cross-sectional length (m)
d	Spray diameter (d)
A_E	Area of the Desired Emitting Flame Surface (m^2)
A_T	Total Flame Surface Area (m^2)
$\dot{Q}''_{rad,1 side of fire}$	Heat Flux at a Target from One Side of the Fire (kW/m^2)

List of Tables

Table 1. Hand calculations of radiation levels from the radiant panel	13
Table 2. Hand calculations of radiation levels from the line burner with propane.....	14
Table B-1. Danfoss 1910 specification [38].	III

List of Figures

Figure 1. Graphical representation of the four mechanisms of droplet breakup from a jet [11]	6
Figure 2. Diagram of the radiation being received by the heat flux gauge from the heat source with a given spray diameter	11
Figure 3. Log scaled unpolarised Intensity vs Scattering Angle plot of a $4.5\mu\text{m}$ wavelength through a $28\mu\text{m}$ droplet.	16
Figure 4. Overlapped $28\mu\text{m}$ MiePlot log scaled polar plot of Intensity vs Scattering Angle comparing Segelstein and Ray refractive indices	17
Figure 5. Overlapped log MiePlot polar plot of Intensity vs Scattering Angle comparing $10\mu\text{m}$, $28\mu\text{m}$, $45\mu\text{m}$, and $80\mu\text{m}$ diameter droplets	17
Figure 6. Log-Log plot of Droplet Diameter vs Forward Scattered Intensity	18
Figure 7. Photo of the water mist column from the Danfoss 1910 hollow cone micro nozzle after activation [2]	23
Figure 8. Velocity and droplet distribution within the water spray [2]	25
Figure 9. Laboratory layout with water mist components attached to a moveable structure	26
Figure 10. Radiant panel baseline measurement setup	27
Figure 11. Diffusion flame line burner baseline measurement setup	27
Figure 12. Radiant panel setup to measure attenuation through various locations within the water mist curtain.	28
Figure 13. Diffusion flame line burner setup to measure attenuation through various locations within the water mist curtain.	28
Figure 14. Radiant panel setup to measure scattering	29
Figure 15. Diffusion flame line burner setup to measure scattering	29
Figure 16. Photo of the water mist curtain activated between the radiant panel and the heat flux gauge.	31
Figure 17. Average radiation attenuation level measured at various heights below the nozzle from the radiant panel	32
Figure 18. Photo of the water mist curtain activated between the diffusion flame line burner and the heat flux gauge	32
Figure 19. Vertically oriented flame average radiation attenuation levels measured at various heights below the nozzle from the diffusion flame line burner	33

Figure 20. Plot of radiation attenuation with the straight line of sight for both radiant heat sources with volumetric concentration levels at various heights within the curtain.....34

Figure A-1 . Danfoss Power Pack PPH 6.3 with a piston pump used throughout the study I

Figure A-2 . Propane radiant panel 0.39 x 0.47 m..... I

Figure A-3 . Line gas burner 0.02 x 0.39 m..... I

Figure C-1. MedTherm 64-5-18 calibration curve V

Foreword

The following report will recap the work done to complete my International Masters of Science in Fire Safety Engineering (IMFSE) thesis here at Lund University; under the supervision of Associate Professor Bjarne Husted from the Department of Fire Safety Engineering at Lund University. The working period for this thesis runs from Jan 25 – May 22, 2015. Submission of the written thesis is due on April 30, 2015 and the thesis defense is May 22, 2015. All work will be conducted here at Lund University.

1. Introduction

During the late 1980's and early 1990's, there were several significant global events that have changed the economic and practical application landscape of water mist system use. Two events in particular were the signing of the Montreal Protocol and the fire aboard the M/S Scandinavian Star. Back in 1987, the Montreal Protocol was signed by 25 [1] countries to phase out the use and production of harmful ozone depleting substances. Since then, more than 191 countries have signed revised editions of that protocol [2]. One of the substances that was found to fall under these restrictions was Halon gas. At the time, Halon gasses were very popular as clean fire suppressant agents. These systems were used in areas where water could do significant damage to compartment contents like computer rooms and archives. After the protocol was signed, alternative methods of extinguishing fires without halon gas needed to be investigated. It was found in the early 1990's that water mist systems were a safe and economical alternative to the Halon systems [3].

Shortly after the signing of the Montreal Protocol, there were several fires on passenger vessels that resulted in large losses of life. One incident in particular was the M/S Scandinavian Star fire in 1990 in-route to Denmark from Norway; 158 passengers were lost that day. These events led the International Maritime Organization (IMO) to rethink passenger safety and fire suppression on vessels traveling through international waters. In 1995, the IMO created regulations that required all ships capable of carrying 35 or more passengers to be equipped with fire sprinklers. These new regulations forced ship designers to find a way of incorporating known traditional fire sprinkler systems. Since traditional fire sprinklers required large amounts of water, and big, heavy piping to successfully control/extinguish a fire, the ships would be extremely top heavy. To combat the risk of capsizing, marine architects looked at utilizing fine spray water mist systems instead. These systems were much lighter, required less water, and took up less space when traveling from one compartment to the next [2, 3].

Due to the above events, there have been several investigative studies into various uses and characterizations of water mist systems ranging from clean agent suppressant alternatives, maritime fire suppression, Class B fuel fire suppression, and compartmentation [1, 3-10]. The later application is of most interest in regards to this study. One of the potential benefits of using water mist as a protective barrier or curtain between a fire and a high value target is its ability to block the transmission of radiation (attenuation). The water mist curtain works by absorbing and scattering radiation electromagnetic waves as they travel through the mist cloud.

After conducting a literature review, it was found that there is very little experimental research on the topic of radiation attenuation through a water mist curtain. The remainder of this report will provide a detailed literature review, a theoretical approach to determining radiative heat transfer through water droplets, a review of previously completed studies on radiation attenuation, the author's experimental design, and a discussion on the results found by the author.

1.1 Objectives

The goal of this study is to provide the first ever experimental radiation attenuation data through a single water mist spray at high pressure and low water flow. The effects of various radiant heat sources on attenuation levels at various heights within the mist column are studied. Finally, the radiation will be measured at various angles with respect to the vertical plane to understand the effects of radiation scattering by the water particles in the forward direction. These results are intended to be used as pilot data for other researchers and to validate future theoretical models and Computational Fluid Dynamic simulations conducted by the scientific community.

1.2 Limitations

Time is the most prominent limitation in regards to completing this project. Having only 3 months to design, build, and conduct experiments can be challenging. Another limitation is the availability of the equipment needed to produce the water mist. At the beginning of this semester, the university did not own or possess the needed pumps, hoses, and/or nozzles. Without the water mist equipment, the attenuation cannot be measured and the protective nature of water mist curtains cannot be assessed. Lastly, the scenarios in the lab are not 100% realistic to the real world environment. There is no way to fully understand the true radiation attenuation capacity of water mist curtains without doing full scale tests with realistic radiation sources and environmental conditions. Therefore, the data gained from this study can only be directly applied to small scale scenarios, but the data can be used as a starting point to understanding larger scale scenarios.

2. Literature Review

2.1 Water Mist Systems

With the increased popularity of water mist systems being used in fire protection designs, it is important to understand what these systems consist of and how they are characterized. Unlike traditional sprinkler systems, water mist systems use a fraction of the water needed to suppress/control a fire; resulting in less water damage to the room contents and property [4]. Also, the piping used is much smaller in size which results in less weight added to the structure and is less noticeable to the occupants.

Water mist system applications can be broken down into three basic types: total compartmentation, local application, and zoned application. Total compartmentation systems have nozzles that are distributed throughout the entire compartment, every nozzle is open, and water will flow through all of the nozzles when an external detection system is activated. This system is intended to fill the entire compartment with a fine mist of water. Local application systems are designed to surround and have their sprays directed towards a specific piece of equipment (i.e. turbine) or potentially hazardous item(s). When activated, this system will suppress a fire only in that one spot in an attempt to protect the surrounding environment. Zoned application systems are designed to protect a specific region within an enclosure. Much like total compartmentation systems, zoned systems will completely fill a particular region with a fine mist while using less water than a total compartmentation system [1 ,3].

Another way to characterize the water mist system is by how the mist is generated: single fluid or twin fluid being the most popular methods. The simplest method (which is used in this study) utilizes only one fluid. The fluid travels through the piping and reaches the nozzle before flowing out of a small orifice in the nozzle and atomizing. The atomization is typically achieved due to the increased dynamic pressure from the ambient air on the fluid jet as a result of the differences in relative velocity between the fluid and the surrounding air. The other method of atomization is by having the fluid impact an obstacle at high velocity. In twin fluid systems, one fluid is the water and the other is a compressed gas (i.e. air, nitrogen, etc.). Inside the nozzle, the compressed gas is positioned in such a way that its spray will flow into the water and cause it to scatter. These twin fluid systems are more complex, more expensive, and require twice as much piping [3].

A third and final way to describe a water mist system is by the level of pressure that the system operates: low pressure (below 12 bar), intermediate (12-34 bar) and high pressure systems (34 bar and above). As the pressure of the system increases, the components need to

exceed the operating pressures, and the methods of providing the needed pressure are different. At lower pressure, centrifugal pumps (like those used by traditional sprinkler systems) are capable of providing the needed pressures for the system. At high pressures, the water can either be supplied by gas driven or pump driven systems. Gas driven system consist of a standalone water tank in a metal cylinder connected to a high pressure gas. When the system is activated, the high pressure gas is fed into the water tank and pushes the water through the piping. The typical operating pressures for this type of system starts around 140 bar and decrease to 30-50 bar. The high pressure pump systems typically contain multiple positive displacement pumps that work in tandem, depending on the number of nozzles that activate, to provide the needed pressure and water flow [3].

Understanding the downstream components of a water mist system is just as important as the pressure generating end. The nozzles used for these systems are as unique as the companies that make them. Their design depends on the operating pressure, the desired application, and the method used to generate the mist (single or twin fluid). Single fluid nozzles can atomize a liquid into a fan spray, hollow cone, full/solid cone, or even a square spray. These sprays are created within a nozzle by a simple orifice, a pre-swirl chamber, a rotating element that spins the fluid, or directionalizing grooves just to name a few. Twin fluid nozzles have an even more complex interior to atomize a fluid than single fluid atomizers. Their interior design consists of two separate channels that converge at the tip in order for the two fluids to collide [11].

2.2 Droplet Formation and Characterization

The size of the water droplets generated by a suppression system is what defines the system as either a water mist system or a traditional sprinkler system. The fire protection community says that systems that generate a spray with 99% of the droplets at 1000 μm or smaller to be considered a water mist system [3]; any system that generates droplet distributions larger than that size and percent are considered traditional sprinkler systems. Previous studies on both theoretical models and experiments have shown that the droplet size is one of several factors that play a role in the amount of radiation attenuated [12-20]. Because of these findings, it is important to have an understanding of how these droplets are formed and characterized.

Although there are several ways to form/atomize a stream of water into fine droplets, (“pressure swirl”, flash vaporization, twin fluid impaction, or obstacle impaction, etc.) this study will utilize pressure atomization. This process works by taking a high pressure stream of water and forcing it through a small orifice to form the droplets. With this approach, four

distinct mechanisms will influence the droplet size and the time of formation after leaving the orifice; which is explained by Lefebvre's book Atomization and Sprays [11]:

- “Rayleigh jet breakup” – The droplets are formed as the fluid jet begins to naturally oscillate due to the surface tension of the fluid. The oscillations reach a point where the forces generated by the fluid's movement are larger than the surface tension, forming droplets that have a diameter larger than the jet. This mechanism forms the droplets the furthest away from the orifice compared to the other three.
- “First wind-induced breakup” – This mechanism introduces the first signs of the atomization process being influenced by the dynamic pressure generated by the ambient air as a result of the difference in relative velocities between the fluid and the ambient gases; along with the oscillations created by the surface tension. This interaction induces increased pressure distributions across the jet and enhances droplet formation. These droplets still form far from the orifice and have a diameter that is roughly the diameter of the jet.
- “Second wind-induced breakup” – As the difference in dynamic pressure between the fluid jet and the ambient gases increase, the jet begins to form as a uniform wavelength instead of simple oscillations. These wavelengths are inhibited by the surface tension of the fluid and pressure buildup, and breakup occurs closer to the orifice. The droplets now have a diameter that is smaller than the fluid jet.
- “Atomization” – This final mechanism occurs right at the exit of the orifice. The droplets are now many times smaller in size compared to the jet.

Each of these four mechanisms can be characterized by the initial amount of turbulence in the jet itself by two parameters: Reynolds number (RE) and Ohnesorge number (Oh). The Oh number is a constant value, representative of a given fluid, which is a ratio of the jet's viscous forces over the surface tension. Figure 1 shows that as the RE number increases (i.e. increase the turbulence) for a given fluid, the droplet formation mechanism shifts right from a “Rayleigh jet breakup” to “atomization”. The water mist system used in this study will generate droplets from the nozzle via the “atomization” mechanism.

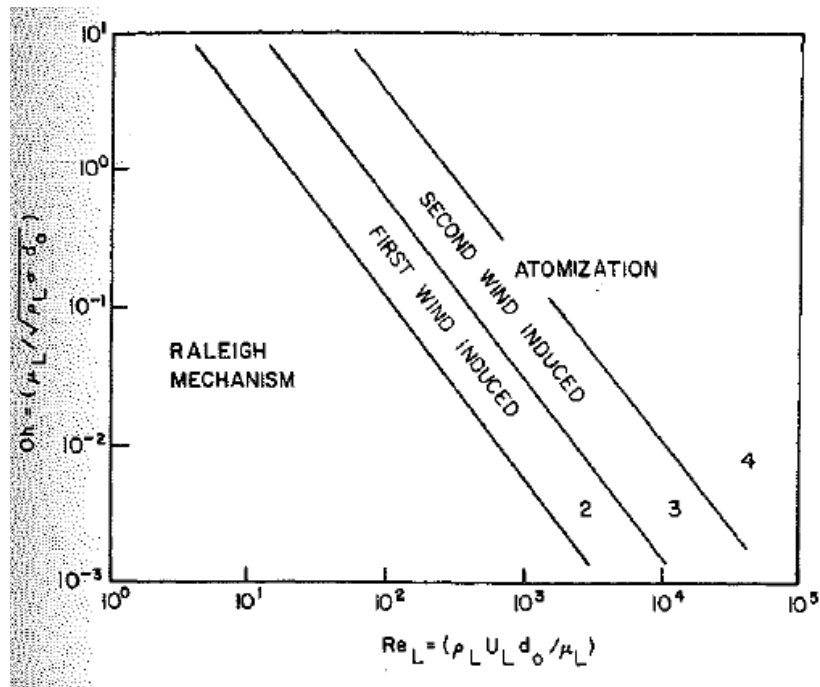


Figure 1. Graphical representation of the four mechanisms of droplet breakup from a jet [11]

Now that it is known how the droplets are formed, it is important to understand the various methods of characterizing the mean diameter of the droplet and how each value can be used. D_{10} is the mean diameter based on the mean size or length of the droplets. This is typically used for direct comparison between droplet sizes. D_{20} characterizes the mean diameter based on the mean surface area of the droplets and is used for surface area controlling. D_{32} is the Sauter mean diameter and is the ratio of the sum of the droplet volumes divided by the sum of the droplet surface area. This is used when calculating mass transfer and understanding the reaction process. The most pertinent mean diameter for understanding radiation attenuation is the D_{30} or D_v ; which is the mean diameter of the droplets based on the mean droplet volume within the spray [11]. Since the volumetric water concentration within the spray is an important characteristic in radiation attenuation, D_v values provide the best distribution of droplet sizes for attenuation analysis.

2.3 How Water Mist Systems Work

Understanding the basic mechanisms of how water mist systems work is not only of interest to the academic community. Firefighters, fire protection engineers, legislators, and international/national code writers, for example, must understand how these systems extinguish and interact with fire within a compartment, on a ship, or out in the open. Several Fire Service lay articles have been written about the use of water mist systems and their effect on occupants, buildings, and firefighting activities [1, 4-10, 21].

Lay journal references [1, 3, 5, 6, 7, 9, 21] all mention that there are three basic mechanisms that water mist systems utilize when extinguishing or suppressing a fire. The first mechanism being the mist's ability to cool the hot gaseous byproducts of combustion and by entrainment into the fire. As the mist interacts with the hot gases and is pulled into the fire plume, it begins to absorb heat, decrease combustion efficiency, and expand into steam. As the flames and hot gases start to cool, the radiant feedback to the fuel source begins to lessen, and the pyrolysis rate of the fuel sources in the compartment slow down.

The second mechanism of extinguishment is the mist's ability to decrease the oxygen concentration and dilute the flammable vapors throughout the compartment. As the mist evaporates, it expands at a rate of 1:1700 (1 L of water → 1700 L of steam). This extreme expansion of steam starts to push the oxygen out of the compartment and dilutes the flammable vapors with water vapor below their Lower Flammability Limits. With less oxygen for the fire to consume and low flammable vapor concentrations to burn, the fire starts to die down and potentially extinguish.

The final mechanism is the mist's ability to block the transmission of radiation from the fire to other fuel sources within the compartment, otherwise known as radiation attenuation. Water mist applications have been described as being able to block the radiation in two different ways. First through a process called "wetting". As the water mist starts to settle within the compartment, it begins to form a thin layer of water on the objects in the compartment. As the radiation reaches the objects, the layer of water absorbs the energy, begins to heat up, and keeps the objects cooled. The second method being the scattering and absorption of the radiation's electromagnetic waves as they move through the mist. The incident radiation weakens as it travels through the mist and hits the target with a lower intensity. One application of particular interest is the use of water mist systems as a protective curtain. This later method of radiation attenuation has been the subject of several theoretical and a few experimental studies over the last 20 years as a means of thermal protection and compartmentation.

2.3.1 Theoretical Research

Several theoretical studies have been conducted to investigate the radiative heat transfer through a water spray. These studies vary from computational fluid dynamic simulations [22, 23, 24], complex scattering and absorption analysis [25], numerical calculations of the radiation transfer equation with Mie scattering theory [13, 19, 15, 26] to simplified 2 flux models [18, 20, 27] and have been validated with experimental results described in Section 2.3.2. Even

though there are several different methods to understand the attenuation of radiation through a water spray, they have come to very similar conclusions.

Their findings show that there are three key parameters that affect the attenuation through the water mist: droplet size, volumetric concentration of the water droplets, and residency time of the droplets through a given volume. As the droplet diameter gets smaller, without changing the flow rate, the attenuation increases. The most efficient droplet size in attenuating the radiation was found to be the same size as the incident wavelength [18, 20]. By increasing the flow rate from the nozzle, or increasing the available volumetric concentration, the attenuation also increased. One study found that the attenuation through the mist at various vertical locations below the nozzle did not change near the nozzle [23], but others said it might vary and even increase as you travel downward [15, 24]. Boulet, et al. 2006 [15], and Collin, et al. 2010 [24], argue that even though the volumetric water concentration decreases as you travel down the curtain, the spray gets wider and the residency time of the droplets increase; resulting in an increase in attenuation. Studies that investigated the width of the spray (in-between the heat source and the target) found that as the width increased, the attenuation increased as well [16, 19, 22]. As a result of adding additional nozzles to increase the width, the velocity and position characteristics of the individual droplets became more complex and the models tended to over predict the attenuation levels.

2.3.2 Experimental Research

After an extensive literature review, there are only a handful of academic studies that investigate the radiation attenuation phenomenon with experimental research. These studies look at a wide range of water sprays: large droplets, fine mists, fan nozzles, hollow cone, and full cone sprays.

Reischl [28] investigated firefighter protection from radiation by using firefighter nozzle sprays as a shield. This project used three different types of firefighting fog nozzles at different spray angles (30°, 60°, and 90°) which operated at two different flow rates (85 and 95 gal/min, or 321.8 and 359.6 L/min respectively). The radiant heat source was a large liquid propane fire with a reflective shield behind it to increase the radiation towards the testing equipment. The nozzles were mounted to a platform with a radiometer attached behind the nozzle at the firefighter position. It was found that the 90° spray was the most effective at attenuating the radiation at ≈13%. Both the 60° and 90° sprays were capable of protecting three to four firefighters, but the 30° spray was found to only be able to protect one fireman. These results provide a good baseline of what large droplet water sprays are capable of attenuating,

but this study did not provide any information about the actual droplet sizes or water concentration in a given volume.

The first experimental studies of radiation transmission through water sprays generated by sprinklers date back to the 1960's. In particular, the study by Heselden and Hinkley [29] looked at the radiation transmission through two downward facing nozzles (fan spray and traditional sprinkler head) placed between a heat source and a radiometer (fan spray)/pyrometer (traditional sprinkler head). They utilized a gas radiant panel for both nozzles at about 800-850°C. Their results show that as the pressure at the nozzle increased, the attenuation of radiation increased. At the same time when the pressure is kept the same and the flow rate increases, the radiation increases. At 3 gal/ft/min (0.75 L/m/min), 50-55% of the radiation was absorbed and at 4-5 gal/ft/min (0.99 – 1.24 L/m/min) 60-70% of the radiation was absorbed. This study did not include droplet size distributions. From the atomization theory explained earlier, as the pressure in the spray increases the droplets become smaller and are more effective.

Three experimental studies were found that looked at radiation attenuation through a single water mist curtain. Work by Parent et.al. [30] looked at transmission of wavelengths through a Tee-Jet 400 067 nozzle at wavelengths between 1.43 μm – 10 μm at lower pressures (1.5 – 6 bar) and low flow rates (0.26 – 0.5 L/min) using a Fourier transform spectrometer. Transmittance was calculated by taking the ratio of received levels with water divided by received levels without water. The spectrometer readings were taken at 20, 40, and 60 cm below the nozzle and at various angles along the horizontal plane. The Sauter mean diameter was found to be 182 μm . They found that there were no significant changes in the transmittance readings between the three vertical positions within the spray. By changing the angle of the detector laterally from the normal direction, the measured intensity decreased rapidly with a small increase in angle. As the pressure increased from 1.5 bar, there was a decrease in transmission until about 4 bar; at 4 bar and above, the transmission levels began to level out and remain approximately 84% or 16% attenuation. It was found that the droplet Sauter mean diameter decreased with the increased pressure resulting in lower transmission. At the same time the injection speed increases; which decreases the residency time of the droplets. All of these aforementioned characteristics will change the attenuation levels.

A similar study utilizing Fourier transform spectrometry was conducted by Dembele et.al. [14]. Dembele utilized two solid cone nozzles that generate a circular pattern: TG03 and TG05. TG05 has the higher flow rate and the largest droplet sizes of the two. As previous studies, the intensity of the laser was measured before and during water activation. Each nozzle

was tested at low pressure from 1 – 7 bar. For the TG05 nozzle, the $D_{v0.5}$ were 550, 375, 300, and 220 μm at 1, 3, 5, and 7 bar, respectively. It was found that the smaller droplets were more effective at decreasing transmission. Similar to the results by Parent et.al. [30], the vertical position of the measurement had minimal effect on the transmission levels (200, 300, and 350 mm below the nozzle). Dembele found that the transmission decreased from 90% to 66% when the flow rate increased from 0.14 L/min to 0.33 L/min, but he states that the distribution of the droplets in the spray is more important than the amount of water in a given volume. In terms of the scattering of radiation away from the normal direction, above 3.5° latterly from the normal, the transmittance is less than 0.1%.

Lastly, a study conducted by Murrell et.al [12] looked at the attenuation of radiation from a gas fueled radiant panel through various water sprays along the normal propagation path. Radiation levels were measured using a Medtherm heat flux gauge. This study also utilizes a lower pressure system operating from 1 – 8 bar with three full cone nozzles (0.52 (A), 1.88 (B), and 4.7 (D) L/min at 3 bar) and one hollow cone nozzle (2.08 (C) L/min at 3 bar). $D_{v0.5}$ ranged from 63 – 171 μm for the hollow cone and 93 – 794 μm for the full cone nozzles. Their results showed that as the pressure increased, the attenuation also increased to a maximum: A-13.9%, B-14.9%, C-30.7%, and D-35.5%. It can also be seen that as the water flow between nozzles A, B, and D increases, so does the attenuation. Lastly, as the droplet diameter decreases, the attenuation increases. They claim that the best combinations of parameters to block radiation is with a spray that has small droplets, low droplet velocity, and high flowrate or high water concentration in a given volume.

The following report will present the first experimental data of radiation attenuation through a single spray water mist curtain at high pressure (100 bar) and low water flow (0.42 L/min), while utilizing both a radiant panel and a gas diffusion flame as radiant sources.

3. Theoretical Calculation Approach for Radiation and Scattering

3.1 Radiation Calculation

In order to determine what heat flux gauges and approximate separation distances to use, simple theoretical calculations are conducted to gain a better understanding of the radiation heat flux levels we could expect from the available radiant heat sources. First, the percentage of radiation attenuation equation is defined (Equation (1)) [24]. Attenuation percentage of the entire radiative heat flux is the measured amount of radiation with water mist divided by the amount of radiation measured without water mist. This resulting value provides the amount of radiation that is blocked by the curtain.

$$Attenuation = 1 - \frac{\dot{Q}''_{rad,with\ mist(H2O)}}{\dot{Q}''_{rad,w/o\ mist(H2O)}} \quad (1)$$

Due to the experimental setup (described in Section 4.2) used during this study, the measured radiation values with and without the water mist used in Equation (1) have to represent the radiation rays that pass through the water mist only. As seen in Figure 2, the heat source is wider than the spray. The orange region denotes the radiation rays that hit the spray and the rays that are captured by the heat flux gauge after passing through the spray. The grey regions are the radiation rays that are unimpeded by the spray. Depending on the diameter of the spray footprint, the amount of unimpeded radiation will vary.

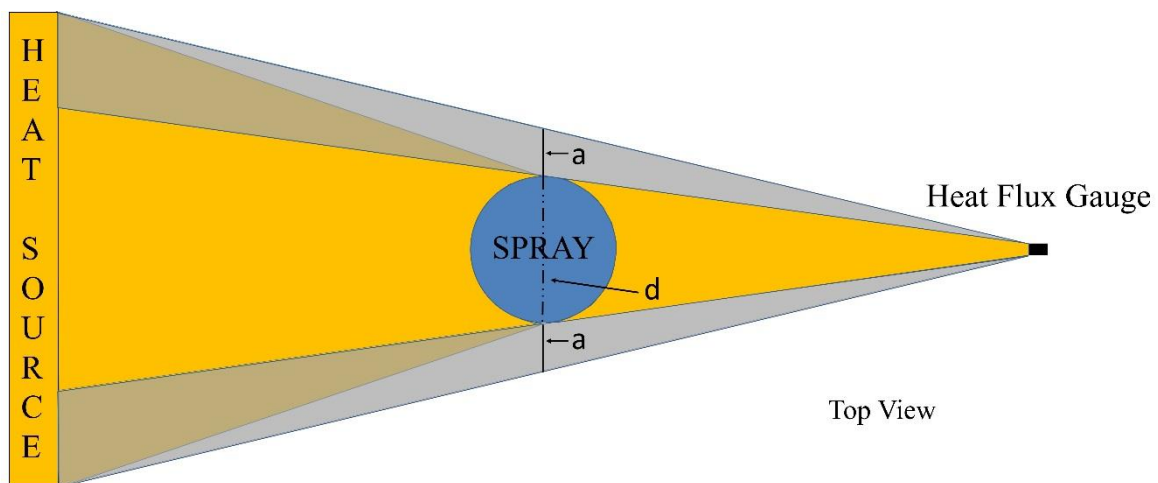


Figure 2. Diagram of the radiation being received by the heat flux gauge from the heat source with a given spray diameter

Since the heat flux gauge used for the below experiments has a view field of 180°, radiation from the surrounds, unimpeded radiation, and radiation passing through the spray will be received. To account for the radiation that does not travel through the spray, the ambient heat flux is assumed to be zero and the unimpeded radiation (grey region) is subtracted from the initial total received flux.

In order to accurately calculate the attenuation from only the radiation waves that pass through the spray, the following calculation steps need to be followed. First, the total measured radiation without water spray is proportionalized based on the cross-sectional length of unimpeded radiation ($2*a$ in Figure 2) (Equation (2)) and the cross-sectional length of radiation through the spray (d in Figure 2) (Equation (3)) divided by the overall cross-sectional length through the center of the spray ($a+a+d$).

$$\dot{Q}''_{rad,w/o\ mist(unimpeded)} = \dot{Q}''_{total\ rad,w/o\ mist} * \frac{2 * a}{(2 * a) + d} \quad (2)$$

$$\dot{Q}''_{rad,w/o\ mist(H2O)} = \dot{Q}''_{total\ rad,w/o\ mist} * \frac{d}{(2 * a) + d} \quad (3)$$

For example, the spray has a footprint diameter of 120 mm and the overall cross-section length that the heat flux gauge views at that location is 187 mm. Taking the ratio of 120/187, this gives the fraction of radiation that will go through the spray and be received by the heat flux gauge (i.e. measured radiation *without* water mist). Once both initial proportionalized radiation levels are found, the total radiation measured *with* water mist is subtracted by the unimpeded fraction of the total measured radiation *without* water mist; resulting in the measured radiation *with* water mist for the rays that pass through the water mist (Equation (4)).

$$\dot{Q}''_{rad,with\ mist(H2O)} = \dot{Q}''_{total\ rad,with\ mist} - \dot{Q}''_{rad,w/o\ mist(unimpeded)} \quad (4)$$

These two values (Equations (3) and (4)) are then placed in Equation (1) to find the attenuation through the water mist curtain.

The radiation given off by a radiant panel was calculated by using Equation (5). It is assumed that the panel is a perfect emitter and the $\epsilon = 1$, with the Stefan-Boltzmann constant $\sigma = 5.67 \times 10^{-5} \text{ kW/m}^2.\text{K}^4$. The view factor (F) was calculated using the technique in Chapter 2 of Drysdale's book [31]; specifically using Table 2.8.

Table 1 provides the radiation levels at a target at various separation distances and various heat source temperatures based on Equation (5)

$$\dot{Q}''_{rad} = F * \varepsilon * \sigma * (T_{panel}^4 - T_{amb}^4) \quad (5)$$

Table 1. Hand calculations of radiation levels from the radiant panel

Target \dot{Q}''_{rad} (kW/m ²) from the Radiant Panel				
Separation (m)	650°C	700°C	750°C	800°C
0.4	10.7	13.2	16.2	19.6
0.5	7.6	9.4	11.5	13.9
0.6	5.6	6.9	8.4	10.2
0.7	4.4	5.4	6.6	8.0
0.8	3.5	4.3	5.3	6.4
0.9	2.8	3.4	4.2	5.1
1	2.2	2.8	3.4	4.1

Similar calculations are also performed for the diffusion flame line burner. Equation (6) and (7) from Karlsson and Quintiere's book [32] are used to find the radiative heat flux at a target from a line burner. To calculate the radiation portion of the heat flux from the fire, the heat release rate of the fire (\dot{Q}) is divided by the total surface area of the flame (A_T) and multiplied by the radiative fraction for propane ($\chi = 0.3$).

$$\dot{Q}''_{rad} = \frac{\dot{Q}}{A_T} * \chi \quad (6)$$

$$\dot{Q}''_{rad,1\ side\ of\ fire} = \dot{Q}''_{rad} * \frac{A_E}{A_T} * F \quad (7)$$

For the purposes of this study, the radiation is being emitted from only one side of the fire. To account for this assumption, the radiative heat flux \dot{Q}''_{rad} is adjusted based on the transmitting area; assuming that the fire is a rectangular prism. The surface area of one side of the prism (A_E) is divided by the total flame surface area (A_T); which results in a ratio that is multiplied by \dot{Q}''_{rad} . Lastly, the view factor (F) needs to be multiplied in order to find the radiative heat flux at the target. The view factor (F) for the line burner is found the same way as described above for the radiant panel. For the line burner, the theoretical flame height is used to define

the parameters needed to determine F. The flame height from the line burner was calculated using Equation (8) [32] to determine the surface area of the prism: L is the flame height, B is the longer dimension of the burner and \dot{Q} is the total heat release rate.

$$L = 0.035 * \left(\frac{\dot{Q}}{B}\right)^{2/3} \quad (8)$$

Table 2 is the resulting radiant heat flux levels received by a target at various distance from the fire and various fire sizes for propane gas.

Table 2. Hand calculations of radiation levels from the line burner with propane

Target \dot{Q}''_{rad} (kW/m ²) from the Line Burner					
	Fire Size (kW)				
Separation (m)	30	35	40	46	48
0.4	2.5	2.7	3.0	3.3	3.4
0.5	1.8	2.0	2.2	2.5	2.6
0.6	1.3	1.5	1.7	1.9	2.0
0.7	1.0	1.2	1.3	1.5	1.6
0.8	0.8	1.0	1.1	1.2	1.3

In order to theoretically determine the attenuation of radiation, the radiation transfer equation (RTE) through a medium needs to be solved. Equation (9) is a differential representation of a modified Lambert-Beers law on radiation intensity within a given volume (S); which in this case is for a single, spherical water droplet [33]. The baseline Lambert-Beers equation does not account for the influence of scattering when calculating the intensity. The below equation adds a scattering coefficient to account for this phenomenon. To simplify the incident and exit radiation through the droplet, only two incoming intensity levels and one outgoing intensity are assumed.

$$\frac{di(\lambda, S)}{dS} = -(K_a(\lambda, S) + K_s(\lambda, S)) * i(\lambda) + K_a(\lambda, S) * i_b(\lambda) \quad (9)$$

The equation has two distinct portions: the absorption (K_a) and scattering (K_s) of the radiation from normal intensity (i), and the emission of radiation from the droplet as a black body (i_b) for a given wavelength (λ) and volume (S). The scattering coefficient (K_s) can be a difficult value to quantify; which makes the RTE very computationally costly to solve. Since K_s is so

difficult to solve, an absorption and scattering program called MiePlot will be used to find the solution to the RTE.

It should be noted that most theoretical work that tries to model and simulate radiation attenuation through water mist typically ignore or over-simplify the in-scattering phenomenon within a single droplet and the inter-scattering of radiation between water droplets. The data collected in the below experiments will include this scattering and will likely result in higher attenuation values compared to theoretical works.

3.2 Volumetric Water Concentration

In order to gain an understanding of the volumetric water concentration (kg/m^3) within the spray, a simplified calculation is used (Equation (10)). It is assumed that the spray pattern is a perfect circle (m^2), all of the droplets have the same peak velocity (m/s), and the flow rate (L/min) is constant. Peak droplet velocities along the centerline and spray pattern diameters are taken from Husted's findings and can be found in Section 4.1 [2, 34].

$$\text{Concentration} = \frac{\text{Flow Rate} * \frac{1 \text{ min}}{60 \text{ s}} * \frac{1 \text{ kg}}{1 \text{ L}}}{(\text{Spray Area}) * (\text{Droplet Velocity})} \quad (10)$$

3.3 Mie Scatter

Mie scattering theory is a mathematical approach to understanding the scattering of a single electromagnetic wave interacting with a spherical particle and determining the extinction of that wave as it exits the sphere in all directions. The Mie calculations attempt to solve the complex RTE equation, by incorporating the scattering and absorption characteristics of a spherical droplet and generates the resulting intensity; which can be used to find the attenuation through the droplet. Although there are several programs that can quantify and visually represent the scattering, MiePlot is chosen [35]. MiePlot is capable of investigating the interaction of a single or multiple wavelengths as they interact with a monodispersion or a polydispersion of droplet sizes found in a water mist cloud.

In a report by Försth and Möller, [36] at SP Technical Research Institute of Sweden, have found that for clean and sooty flames the predominant, peak emitted wavelength is $\approx 4.5\text{-}4.8 \mu\text{m}$. The polar plot MiePlot generates is an Intensity vs Scattering Angle with a logarithmic base 10 scaling. Figure 3 shows the unpolarised Mie scattering through a $28 \mu\text{m}$ monodisperse droplet cloud utilizing Segelstein water droplet refractive index. The incident wavelength enters the droplet from the left and exits on the right side. Most of the intensity is scattered in

the normal direction (left to right), but there is evidence that it is also scattered up, down, and backwards. In order to find the amount of radiation that a target will receive, the intensity needs to be multiplied by the fraction of rays viewed by the target. This fraction is found by integrating over a given angular span (grey triangle Figure 3) and then dividing that value by the integral of the intensity over the whole 360° [2]. In reality, the scattering is not planar as seen in the figure. The plot should be visualized as a three dimensional image by rotating about the horizontal axis.

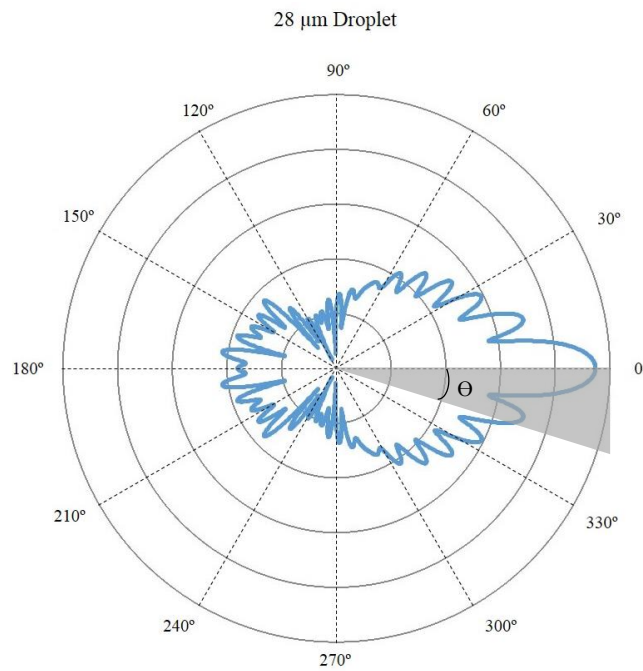


Figure 3. Log scaled unpolarised Intensity vs Scattering Angle plot of a 4.5 μm wavelength through a 28 μm droplet

MiePlot allows for the user to select one of four different sets of refractive indices when it comes to describing how the light source or wavelength bends after entering a spherical water droplets: IAPWS, Segelstein, Ray, and Kaye + Laye. IAPWS and Kaye + Laye indices both cannot be applied for this research, because the applied incident radiation source has a wavelength (4.5 μm) that falls outside their validity ranges. Figure 4 shows the overlapped log polar plots of a 28 μm droplet Intensity vs Scattering Angle comparing Segelstein and Ray refractive index effects. It can be seen that there is an insignificant difference between the two indices in terms of scattering intensity and angular distribution.

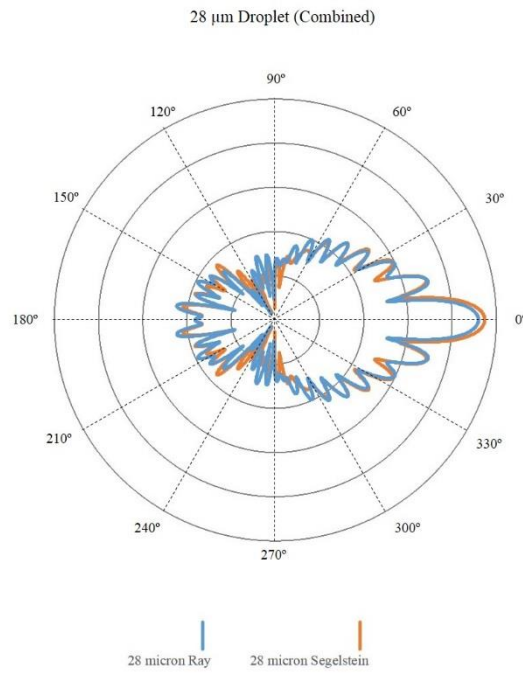


Figure 4. Overlapped 28 μm MiePlot log scaled polar plot of Intensity vs Scattering Angle comparing Segelstein and Ray refractive indices

As explained earlier, the size of the droplet is an important characteristic in determining the attenuation. Figure 5 shows the change in intensity and scattering angle for four different droplet sizes (10, 28, 45, and 80 μm) in a monodispersed cloud being subjected to the same single point source wavelength of 4.5 μm with the Segelstein refractive index.

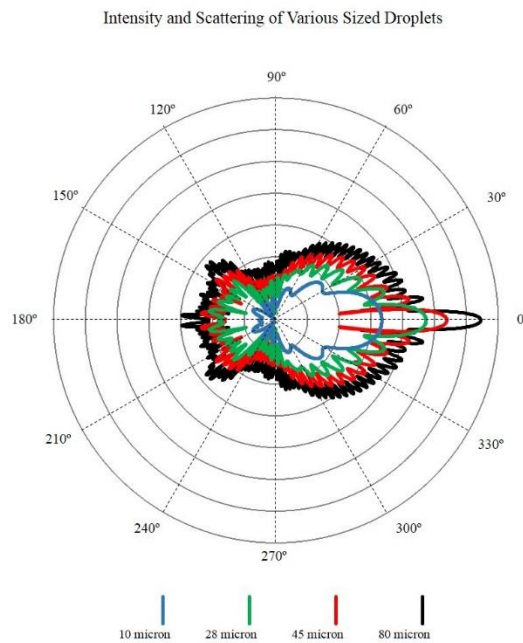


Figure 5. Overlapped log MiePlot polar plot of Intensity vs Scattering Angle comparing 10 μm, 28 μm, 45 μm, and 80 μm diameter droplets

It can be seen that as the droplet diameter decreases, the intensity also decreases. This trend matches those found in the theoretical models, simulations, and experiments. The forward scattering becomes more prominent as the droplet gets larger; meaning that the larger droplets are not as efficient at absorbing and scattering the incident wavelength. On a log-log Droplet Diameter vs Forward Scattering Intensity plot, there is a linear relationship between the two (Figure 6). Overall, the scattering away from normal and backwards maintain the same shape for all droplets. Although the scattering shape remains similar as the droplets get smaller, the variance in the intensity levels over a given degree span lowers. This results in a smoother intensity plot line.

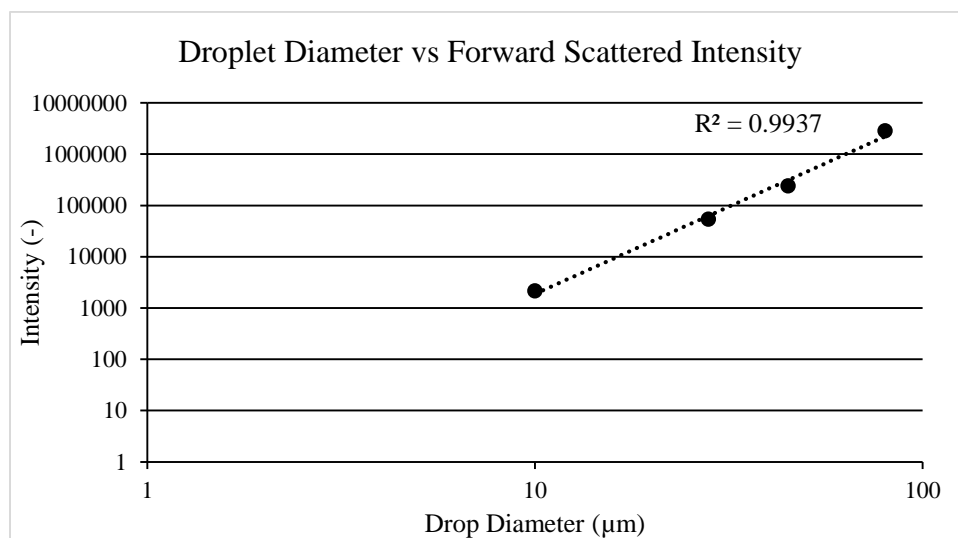


Figure 6. Log-Log plot of Droplet Diameter vs Forward Scattered Intensity

Unfortunately, MiePlot cannot be used in this study as a way of comparing the attenuation levels from the experimental results with a theoretical approach. This is due to the experimental setup and the assumptions that would need to be made in order for MiePlot results to be compared with the experiments. Of these limitations, the most significant is in regards to the way that the radiation is generated. During the experiments the radiation enters the water mist curtain from all different angles: above, below, straight, left, and right (Figure 2). For example, if a radiation ray enters the droplet from above and exits out the bottom, a majority of it is not seen by the heat flux gauge. Now add a ray through the droplet (from the heat source to the heat flux gauge) and the resulting radiation that exits the droplet and seen by the heat flux gauge will no longer be influenced by just one ray but rather all rays entering the droplet. MiePlot on the other hand is limited to only a single point source. Even though multiple rays can be used in MiePlot, they are still generated at a single point and travel horizontally through the droplet. For the experiments to be comparable, a point radiation source would need to be used; like a laser. Another limitation is that the actual water mist curtain that is generated in

the experiment does not consist of only one droplet size. MiePlot is capable of analyzing a mist cloud with a droplet size distribution, but the experimental data is not available to accurately describe the droplet size distribution at all measurement heights.

4. Methodology

In order to generate meaningful results for this thesis, the earlier described experiments in Section 2.3.2 were consulted as a guide in regards to the experimental setup and data collection used here. The experiments being presented by this author are an extension of the work previously conducted by Husted [2] and rely heavily on his results for background information about the water mist characteristics for the tested spray. Because of the amount of time and resources it would require to determine water mist characteristics for a different spray, the same water mist system Husted used will be incorporated here (high operating pressure and low water flow).

As explained above, all of the previous experimental studies have all been low pressure systems with medium to high flow rates. Although these low pressure experiments (1 – 8 bar) provide valuable information and insight into understanding water mist curtains, they may not fully capture all of the information. The SFPE handbook [3] states that low pressure water mist systems typically will have a nozzle pressure between 8 – 12 bar in order to generate the necessary droplet size distribution. To meet water mist system performance requirements, many manufacturers are designing their low pressure systems at pressures ranging from 12 – 20 bar at the nozzle. With most water mist systems in the field operate at higher pressures than previously tested, the water mist may behave differently. This is why it is important to expand the research towards the higher end of the pressure spectrum.

Nozzle orientation was selected to be downward because it needed to match the previously collected mist characteristics. Also, in order to compare the high pressure results with the low pressure results and considering that most water mist systems in the field generate protective curtains with downward oriented nozzles.

To generate the radiation levels needed to ensure strong readings, many different options have previously been used: large liquid propane (LP) fire [28], large wood cribbing fire [37], Fourier transform infrared spectrometer (laser system) [14, 30], gas radiant panel [12, 29]. The first two options, LP and wood cribbing, generate fires that are too large for the lab space available here at Lund University. Utilizing the laser system is the least intrusive method and is the least likely to interact with the water mist curtain. One problem with the laser system is that it can only investigate the attenuation from a single wavelength. Even though a full spectrum of wavelengths can be tested, there is no way to generate the interactions of a variety of wavelengths generated by a diffusion flame at the same time. Unfortunately this equipment is not available for use. The radiant panel provides an acceptable constant radiant heat source,

producing a small band of wavelengths, and is available in the lab. Therefore, a radiant panel will be used for this thesis in order for the results to be compared with previous works. Since none of the above options can be used in our lab space to generate the full spectrum of wavelengths from a diffusion flame, the author will also use a small diffusion flame line burner. This line burner is capable of burning several different gaseous fuels and generating a fuller radiation spectrum. Propane gas will be used in both the radiant panel and the line burner; due to the propane's higher radiative fraction and its availability in the lab. Other gases, like methane, have very lower radiative fractions and the flow rates required to create radiant heat flux levels large enough to be measured are not available in the lab space.

The scattering of radiation away from the forward propagation through a full curtain has received very little attention. The studies that have looked at scattering through a curtain have only investigated the scattering horizontally (left and right of center) [14, 29, 30]. They change the position of the heat flux receiver horizontally from the center and direct it to the center of the heat source to measure the scattering affect. Also, they assume that the scattering is horizontally symmetrical. None of the studies mentioned above look at the forward scattering with respect to the vertical plane of propagation (above and below the forward propagation). Since the vertical symmetry of the scattering in the forward direction has not been studied within a curtain, radiation measurements will be taken along the vertical axis at an angle above and below the forward propagation path.

4.1 Water Mist Characteristics

The water mist used in this study is generated by a Danfoss 1910 single, hollow cone micro nozzle with a spray angle of 60°. This same nozzle was used by Husted [2] during the execution of his PhD thesis and provides the detailed analysis of this mist's characteristics. Figure 7 shows the shape of the water mist spray after activation and stabilization.

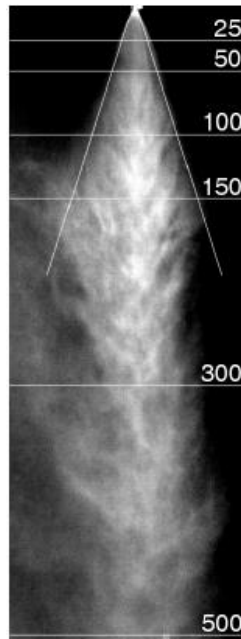


Figure 7. Photo of the water mist column from the Danfoss 1910 hollow cone micro nozzle after activation [2]

There are four distinct regions of interest within the spray. The first region is the initial conical zone from 0 mm to 50 mm. The initial cone consists mainly of high velocity and small $D_{v,0.5}$ water particles as they exit the nozzle. The second zone being the inflow zone around 100 mm. This zone starts to entrain ambient air into the spray and the water particles begin to slow down. This zone is followed by the transition zone below 150 mm. It is around this point that the initial conical shape of the spray begins to fall apart due to gravity and the particles fall straight down with minimal lateral velocity. The final zone is the continuous turbulent zone after 300 mm. Here the distribution of the water particles is the most uniform across the entire circular spray pattern.

When attempting to define the distribution of droplet diameters and velocities within a dense spray, like a water mist curtain, there are a combination of options available. Droplet velocities and diameters can be found using Particle Image Velocimetry (PIV), high speed imaging, or Phase Doppler Anemometry (PDA). Due to the high density nature of the spray, PIV and high speed imaging are not efficient methods of determining the droplet diameters. PIV works by illuminating a planar section of spray with a laser sheet. This laser sheet is then photographed multiple times. The photos are analyzed with post processing software by comparing the pixel intensity between two images and calculates the velocity for the given pixel and not for the particles themselves. High speed imaging works in a similar way as PIV in a sense that the measurements are made on a planar section. Thousands of photographs are taken every second and allows the researcher to track the individual droplets from frame to

frame through the pixels. Post processing of this information is extremely labor intensive on the part of the researcher as there is no software to track droplet movement.

PDA measures the droplet characteristics at a point and not over a plane like PIV and high speed imaging. Two laser beams intersect at a given frequency over a given volume. As the droplets pass through the volume, they scatter the lasers and that scattering is picked up by detectors on the opposite side of the spray. Using a post processing software, based on the received scattered beam intensities and frequencies, the droplet velocity and droplet size can be found. An alternative method of finding the droplet sizes is by laser diffraction. This method is only able to determine droplet size and not velocities. As the droplets pass through the laser beam, the scattered beam passes through Fourier lens within the receiver. The lens project the scattered light onto ring shaped detectors that correspond to a particular diameter. PDA's ability to measure both droplet velocity and diameter at the same time in a dense mist made it the best method available for Husted's water mist experiments. Based on Husted's PDA analysis of the 1910 hollow cone spray, Figure 8 was created and depicts the droplet velocities, size distributions, and spray widths at various locations below and away from the nozzle. It is assumed that after 500 mm below the nozzle, the spray width will remain constant.

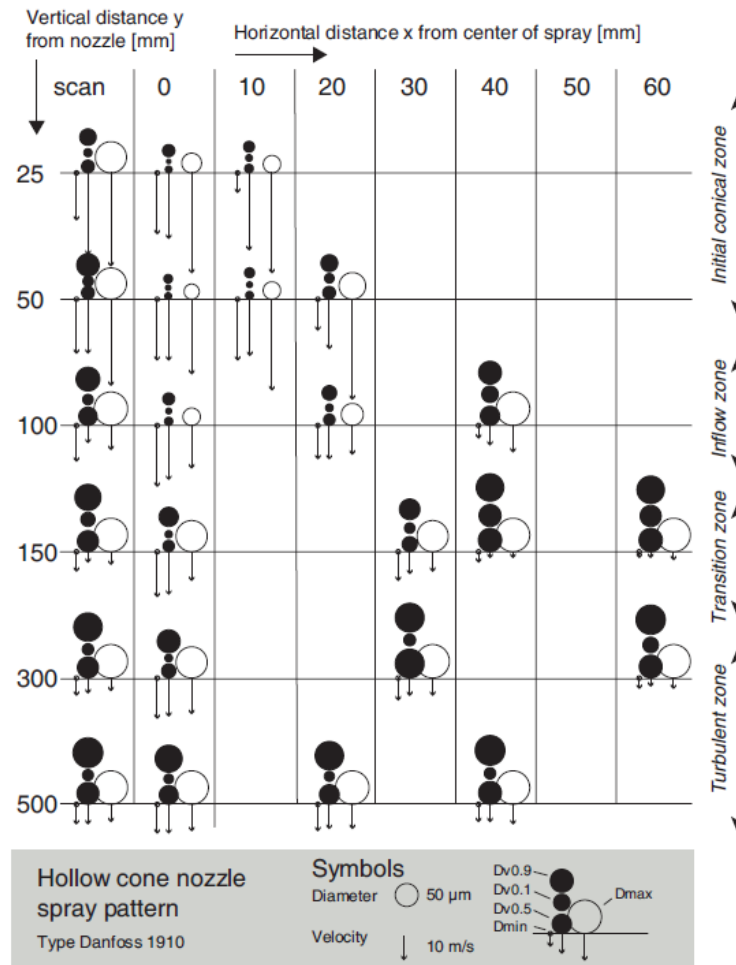


Figure 8. Velocity and droplet distribution within the water spray [2]

Based on the PDA analysis, the $D_{v0.5}$ sizes were found at the following locations below the nozzle: 28 μm (25 mm), 35 μm (50 mm), 40 μm (100 mm), 45 μm (150 mm), and 48 μm (300 and 500 mm) [2]. The peak velocities along the centerline within the spray at various heights are: 33.5 m/s (25 mm), 28.1 m/s (50 mm), 22.1 m/s (100 mm), 19.2 m/s (150 mm), 13.8 m/s (300 mm), 8.4 m/s (500 mm), and 4.6 m/s (700 mm) [34].

A verification study was performed to confirm the water flow data in the Danfoss nozzle literature and it is explained in the Appendix B: Flow Rate Test Procedure. Danfoss [38] states that the water flow through the nozzle under 100 bar operating pressure to be 0.42 L/min. This value was confirmed while utilizing the pump and nozzle setup that will be explained in Section 4.2. If this value were not true, the droplet size distribution assumed in this study would not match the previous work by Husted.

4.2 Experimental Setup/Procedure

4.2.1 Equipment

To provide the high pressure required by the water mist system, a Danfoss Power Pack PPH 6.3 with a piston pump capable of providing 4 L/min under high pressure is utilized (Figure A-1). The pump is connected to a 1 m long stainless steel 12mm \varnothing pipe by a 3m long high pressure hose. At the end of the pipe, a single Danfoss 1910 micro nozzle is directed vertically towards the ground. The water mist piping is attached to an adjustable structure constructed out of extruded aluminum beams. This superstructure is capable of moving the nozzle both vertically and horizontally with respect to the radiant panel/line burner position (Figure 9). Heat flux levels are measured with a MedTherm 64-05-18 water cooled heat flux gauge. It is the author's understanding that the heat flux gauge used is a Gardon type gauge. This means that the convective heat transfer at the surface of the device is not taken into account; therefore, it only receives the radiative flux from the heat source. Before any tests were conducted, the heat flux gauge was calibrated here at Lund University and the calibration curve can be found in Appendix C. MedTherm specifications state that their gauge has a $\pm 3\%$ uncertainty. All data is collected at a frequency of 1 Hz with a dataTaker DT85 Series 2 data logger.

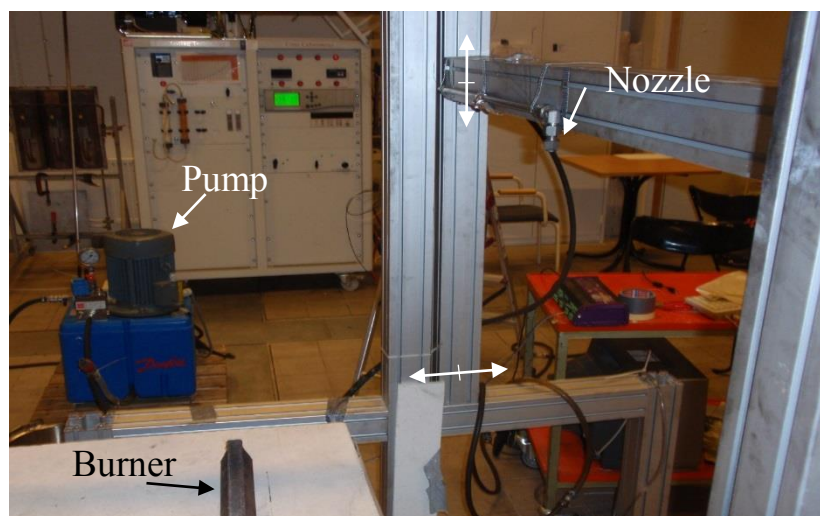


Figure 9. Laboratory layout with water mist components attached to a moveable structure

Two heat sources are used to produce the necessary radiant heat flux needed to measure the attenuation. The first being a propane fueled three burner radiant panel with an emitting surface measuring 0.39 m wide and 0.47 m tall (Figure A-2). The second being a diffusion, gas line burner with a burner area of 0.02 m x 0.39 m (Figure A-3).

4.2.2 Procedure

Both heat source scenarios will follow a similar procedure. A broad step by step procedure can be found in Appendix D: Experimental Procedure; while a brief overview with precise separation distances and measurement locations is described here. Appendix E provides a detailed risk assessment of the experiments and is required by the laboratory facility to be completed before any test can be conducted.

Baseline radiation measurements will be collected before and after every activation of the water mist to ensure there was no decrease in intensity due to decreased flow rates from the small fuel bottle. For the radiant panel, the heat flux gauge will be placed 0.8 m away from the panel and directed towards the center of the emitting surface (Figure 10). The temperature of the radiant panel is $\approx 700^{\circ}\text{C} \pm 50^{\circ}\text{C}$. At this distance, the panel will emit about $3.5 - 5.3 \text{ kW/m}^2$ of radiation (Table 1). The diffusion flame line burner is positioned 0.75 m away from the heat flux gauge. The propane fire size used is supplied with approximately 20 L/min of fuel ($\approx 46 \text{ kW}$); resulting in a theoretical flame height of 0.87 m (Figure 11). The heat flux gauge will be directed at a height of 0.43 m above the burner's surface (or theoretical center of the flame sheet) resulting in $\approx 1.3 \text{ kW/m}^2$ of radiation (Table 2).

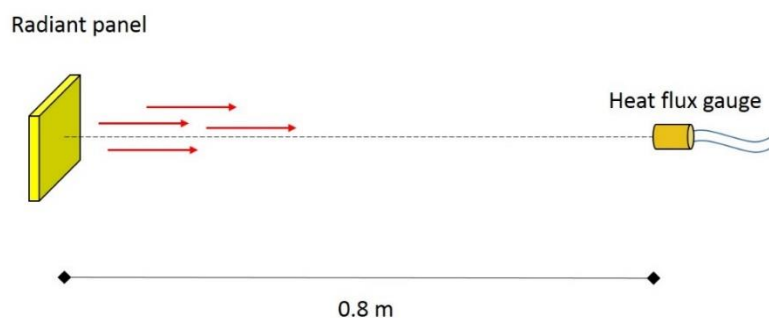


Figure 10. Radiant panel baseline measurement setup

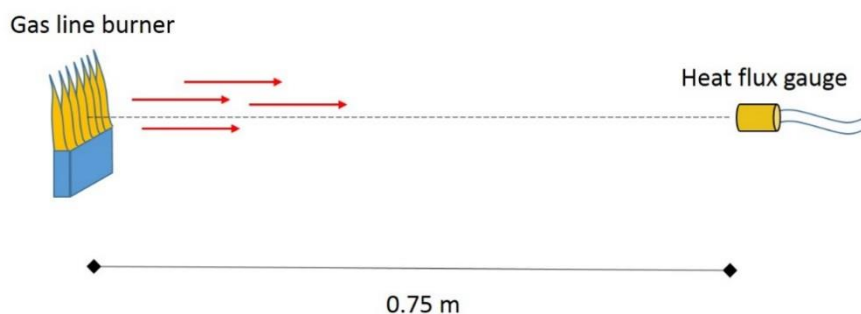


Figure 11. Diffusion flame line burner baseline measurement setup

Radiation levels will be collected at seven different locations below the nozzle: 25, 50, 100, 150, 300, 500, and 700 mm. The nozzle is attached to the aluminum superstructure and will be moved up and down to the desired height while the heat source and the heat flux gauge

heights remain fixed. The water mist curtain is positioned equidistantly (0.4 m) between the radiant panel and the heat flux gauge. For the line burner, the burner will be 0.4 m away from the center of the water mist and the heat flux gauge will be 0.35 m from the water mist column center. Radiation measurements through the water mist will first be made in the normal propagation direction from the heat source (Figure 12 and Figure 13). The “straight line of sight” from the heat flux gauge to the heat source will go through the horizontal center of the water mist curtain.

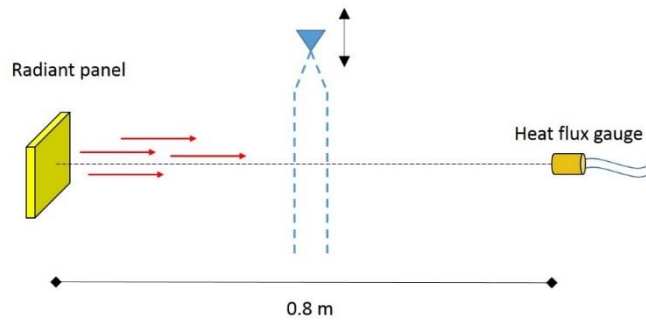


Figure 12. Radiant panel setup to measure attenuation through various locations within the water mist curtain

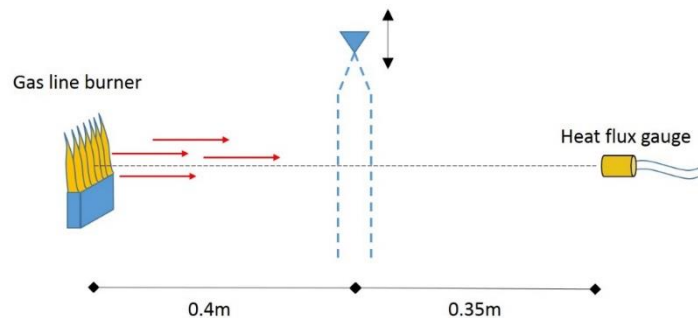


Figure 13. Diffusion flame line burner setup to measure attenuation through various locations within the water mist curtain

Next, without changing the height of the nozzle, the heat flux gauge will move up and down 70 mm and be rotated by $\approx \pm 5^\circ$ to measure the scattering in the forward direction (Figure 14 and Figure 15). Once all three measurements have been taken for a particular location below the nozzle, the superstructure is repositioned to the next desired height within the water mist curtain and the three radiation measurements will be repeated for the remaining nozzle locations.

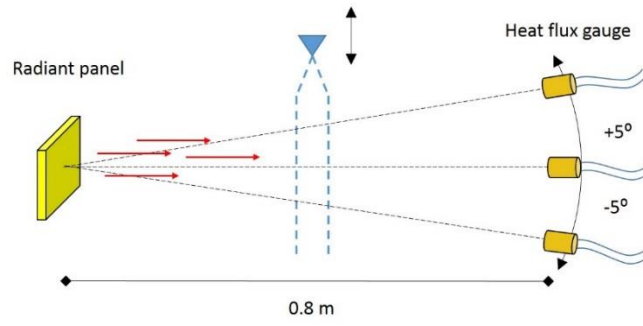


Figure 14. Radiant panel setup to measure scattering

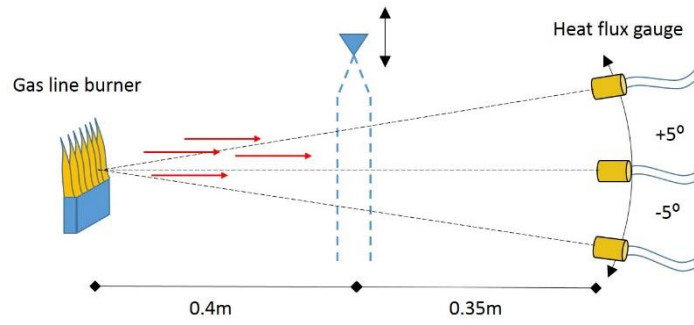


Figure 15. Diffusion flame line burner setup to measure scattering

5. Results

5.1 Radiant Panel

The radiant heat flux generated by the radiant panel had minimal fluctuations during the experiments with and without the water mist curtain. Figure 16 shows the experimental setup with the radiant panel and the water mist activated at one of the lower nozzle position settings.

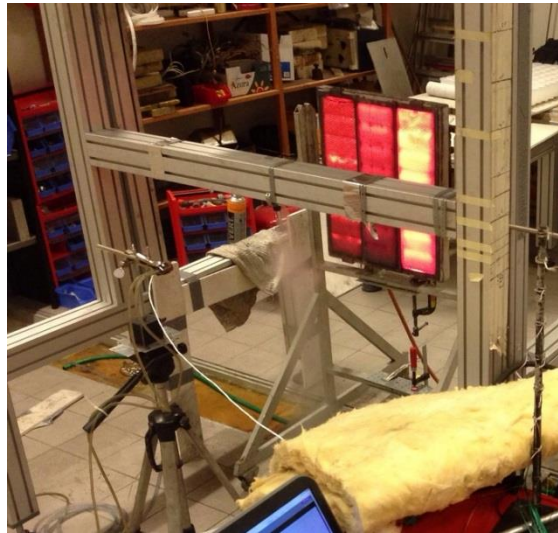


Figure 16. Photo of the water mist curtain activated between the radiant panel and the heat flux gauge

Figure 17 depicts the average radiation attenuation measured through the curtain at the various heights. Average radiation attenuation percentage levels are along the X axis and the position below the nozzle where the data was collected is along the Y axis (zero is the nozzle tip). The blue line represents the calculate values collected with the heat flux gauge pointed along the normal radiative path. The green line represents the calculated values collected with the heat flux gauge looking from above with an angle of 5° . The orange line is the same as the green line but the heat flux gauge is now looking from below up into the water curtain with roughly the same 5° inclination. These values were calculated with Equation (1). It should be noted that the measured incident radiation level *without* water mist was the average of the radiation levels measured before and after water mist operation.

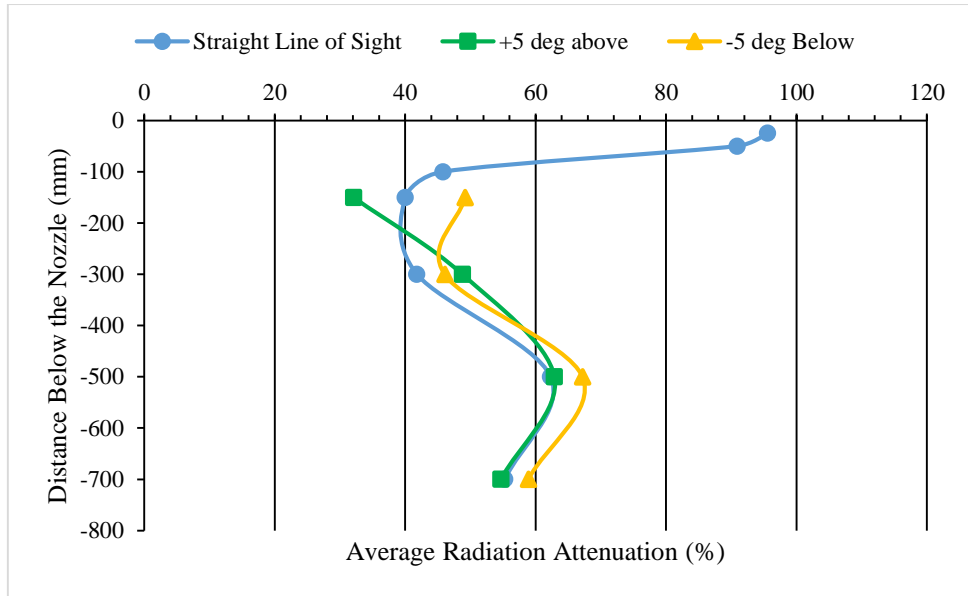


Figure 17. Average radiation attenuation level measured at various heights below the nozzle from the radiant panel

5.2 Diffusion Flame Line Burner

Figure 18 shows the experimental setup with the line burner and the water mist both activated. The radiant heat flux generated by the propane gas line burner fluctuated a lot during the experiments with and without the water mist curtain because the ventilation within the lab forced the flame to shift back and forth. Due to the exhaust system in the lab, the fire tended to be pulled away from the heat flux gauge. When activated, the water mist curtain tended to pull the surrounding air downward with the water and dragged the fire with it toward the heat flux gauge. In the background of Figure 18, the reader will notice the author holding up a board. This board was used to help control the ventilation conditions near the flame and provided a means of keeping the flame in a vertical position with and without water mist.

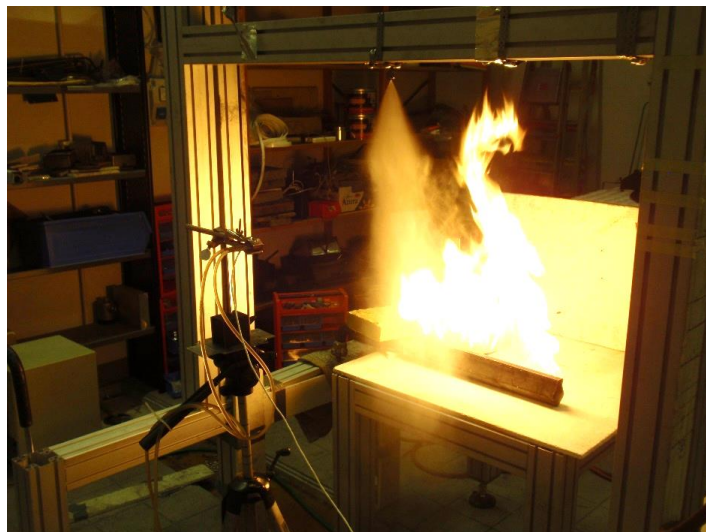


Figure 18. Photo of the water mist curtain activated between the diffusion flame line burner and the heat flux gauge

Even with the board in place to assist in flame position control, the flame still would move towards and away from the heat flux gauge resulting in very high and very low radiation values. To refine the data and lower the variability, during the experiments it was noted when the flame sheet was in the vertical position and the measured radiation levels at those times are used to create the below figure.

Figure 19 is a graph of the average radiation attenuation measured through the curtain at the various heights with the flame sheet in the vertical position. Average radiation attenuation percentage levels are along the X axis and the position below the nozzle where the data was collected is along the Y axis (zero is the nozzle tip). The blue line represents the calculate values collected with the heat flux gauge pointed along the normal radiative path. The green line represents the calculated values collected with the heat flux gauge looking from above with an angle of 5°. The orange line is the same as the green line but the heat flux gauge is now looking from below up into the water curtain with roughly the same 5° inclination. These values were calculated with Equation (1). The author would like to note that there was some interaction between the diffusion flame and water mist curtain at 300, 500, and 700 mm below the nozzle. It should be noted that the measured radiation level *without* water mist was the average of the radiation levels measured before and after water mist operation with the flame in a vertical position.

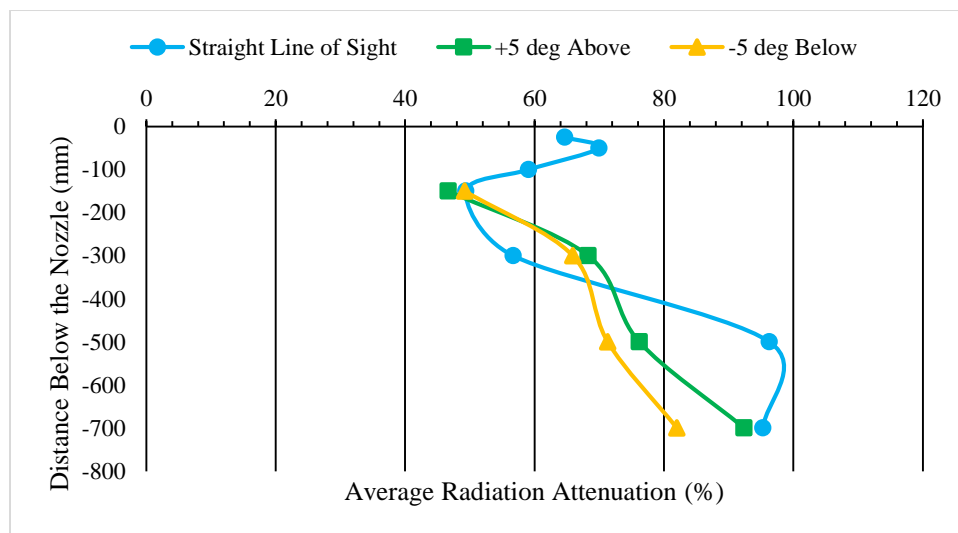


Figure 19. Vertically oriented flame average radiation attenuation levels measured at various heights below the nozzle from the diffusion flame line burner

The volumetric concentration within the spray varies with height below the nozzle just like the attenuation. Figure 20 shows an overlapped plot of the volumetric concentration with the straight line of sight attenuation levels for both the diffusion flame line burner and the radiant panel.

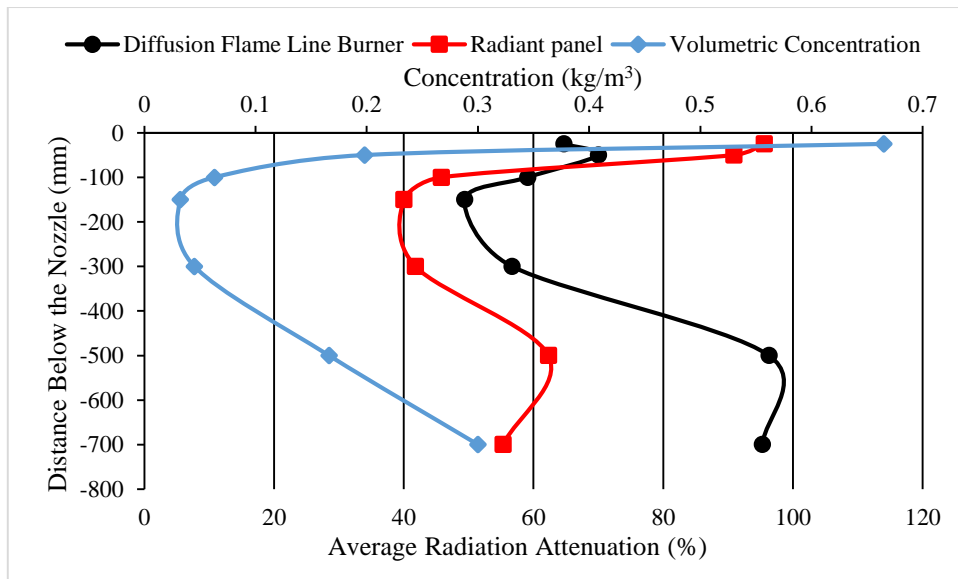


Figure 20. Plot of radiation attenuation with the straight line of sight for both radiant heat sources with volumetric concentration levels at various heights within the curtain

5.3 Uncertainties in the Results

Even though all attempts were made to ensure the accuracy of the results, some uncertainties need to be taken into account when interpreting the results. One obvious source uncertainty is the MedTherm 64-5-18 itself. MedTherm states that the output from the gauge itself has an uncertainty of $\pm 3\%$. The radiant heat flux levels measured during these experiments are lower than what the heat flux gauge is calibrated for; below 5 kW/m^2 (Figure C-1). The calibration line equation is assumed to be representative of these lower values, but in reality this assumption might not be true. Utilizing heat flux gauges with low maximum thresholds would help decrease this uncertainty.

The experimental setup itself is prone to generating errors. Every time the desired measurement position or heat flux angle changes, the heat flux gauge and nozzle move. If the setup is not properly checked, the heat flux gauge could fall out of alignment and might not be pointed directly through the center of the spray or at the center of the heat source. Another uncertainty involving the experimental setup was the heat sources. The radiant panel was unable to produce uniform temperatures across all three burner (See Figure 16). Also, due to the ventilation condition within the lab, the diffusion flame was not always in the vertical position. It tended to move towards and away from the heat flux gauge during the testing. Even the data used to characterize the spray (velocity, spray size, droplet size, and position within the spray) that Husted found might have large variances and for the calculations solved here, only the mean values of that data are used when calculating water concentration.

On the other hand, the flow rate of the fuel into the heat sources and the pressure supplying the nozzle remains the same for all tests. Even with the constant fuel flow rate into the diffusion flame line burner, the ventilation conditions within the lab influenced the flame position and the measured radiation values.

6. Discussion

6.1 Comparison between Theoretical and Experimental Baseline Radiation Levels

On average, the baseline radiation levels measured from the radiant panel are $\approx 4.0\text{-}4.1$ kW/m² with an 80 cm separation and a temperature of $\approx 700^\circ\text{C}$ measured by a thermocouple. Based on the theoretical results found in Table 1 using Equation (5), Section 3.1, at 700°C and 80 cm separation, the radiation should be up at 4.3 kW/m². Given the uncertainties in the heat flux gauge and in the temperature of the radiant panel, that are not able to be accounted for in the theoretical equation, the heat flux values match quite nicely except for the locations 50 mm and 25 mm below the nozzle. These two locations report heat flux values that are 0.9 and 1.0 kW/m² lower than the theoretical values, respectively. These lower values are due to the fact that the crossbar supporting the nozzle and piping block a portion of the radiation viewed by the heat flux gauge; resulting in a different view factor in the theoretical calculations compared to the other locations.

For the diffusion flame line burner, the flame sheet has a tendency to move towards and away from the heat flux gauge even with the water mist turned off. Baseline values would range from 0.2 – 2.0 kW/m². When the flame sheet is in a vertical position, the 46-47 kW fire generates on average 1.1 – 1.4 kW/m² at a distance of 75 cm away from the heat flux gauge. The theoretical values in Table 2, Section 3.1, suggest that the heat flux should be 1.2 – 1.5 kW/m² at that same distance. The theoretical Equations (6) and (7) are not able to take into account the constant movement of the flame. Also, the equations assume a constant ratio of emitting surface area of the flame over the total surface area of the flame. This ratio is not constant in reality. Even with these two factors that cannot be accounted for in the theoretical equations, the theoretical and experimental values are quite similar. Once again, as the measurement locations 100, 50, and 25 mm below the nozzle are taken, the baseline radiation levels decrease to about 1.0 kW/m² because of the crossbar blocks the view of the heat flux gauge. Overall, the theoretical values in Table 1 and Table 2 over predict the baseline radiation values. The theoretical calculations are not able to take into account all of the fluctuations in flame position for the line burner or any unexpected heat losses from the radiant panel that tend to lower the measured heat flux.

6.2 Radiant Panel

When looking at the attenuation data for the straight line of sight data in Figure 17, there is a decrease in attenuation as the droplets get larger further downstream from the nozzle from 96% to 40%. This trend matches what was reported by the theoretical studies. Although the best radiation blocking is near the nozzle, in practice this position will not provide the desired protection. If the entire curtain was constructed out of the 28 μm droplets with a concentration of 0.665 kg/m^3 , then the curtain could provide very high attenuation levels. In reality, the spray from 0 – 100 mm below the nozzle only has a spray width ranging from 20 – 80 mm. With the additional spacing between nozzles, the radiation will not pass through the curtain, but rather over it unimpeded. The attenuation then begins to increase again at 300 mm (42%), peaks at 500 mm (62%), and drops again at 700 mm (55%). Contrary to previous studies that state that the attenuation remains somewhat unchanged when the vertical position within the spray changes, these results show that that conclusion to not be true [14, 30]. Each location measured in the curtain has a unique combination of droplet sizes, concentration, and residency time that absorb and scatter the radiation differently. Because of the uniqueness of the various combinations, the vertical position within the curtain can be an important parameter when designing a water mist curtain.

Coppalle [20] found that the “maximum attenuation efficiency is afforded by drops whose diameter is of the order of the maximum emission wavelength of the source.” As stated before, the assumed incident wavelength is $\approx 4.5\text{-}4.8 \mu\text{m}$; therefore, droplets of magnitude should result in the best attenuation. Even though the volumetric concentration of water and residency time is larger at 700 mm (0.3 kg/m^3) than 500 mm (0.166 kg/m^3), as the droplets get larger towards the bottom of the spray and spread out, they are less affective and a corresponding lower attenuation is reported.

As seen in the orange line, attenuation levels looking from below are higher than the straight line of sight. Based on the Mie polar plots we know that the intensity out of a droplet is strongest in the normal direction and rapidly decreases at all other forward angles. Since the amount of radiation that is scatter at an angle from the normal is lower, it makes sense that the attenuation is greater.

The green line representing the downward line of sight has no distinct trend like the others. Towards the bottom of the curtain the attenuation levels are the same as the straight line of sight. At these positions the water mist curtain is very uniform and the inter-scattering between the droplets could play a factor in explaining why the attenuation levels are the same.

6.3 Diffusion Flame Line Burner

Figure 19 shows the average radiation attenuation values for the vertical diffusion flame. As stated before, the flame had a tendency to move closer and away from the heat flux gauge frequently. Therefore it was important to find the average values when the flame was vertical. Once again, the blue line represents the straight line of sight radiation measurements. Just like the radiant panel results, the attenuation increases as the droplets get smaller from 150 mm to 50 mm below the nozzle. At 25 mm, the attenuation is 5% lower than at 50 mm location. This skew from the trend could be a result of a misalignment of the experimental equipment. Although the author tried to ensure that the heat flux gauge was placed directly in the center of the curtain for a tests, the heat flux gauge could have shifted. Considering that the spray width is 20 mm at exit of the nozzle and the view window on the heat flux gauge is less than 10 mm, a slight misalignment would result in the heat flux gauge receiving extra unimpeded radiation; thus lowering the attenuation. Just as the radiant panel results, as the droplet size gets closer to a magnitude of the wavelength, the attenuation increases. The jump in attenuation between the 300 mm and 500/700 mm positions is twice as large as the radiant panel levels. These extremely high attenuation levels are due to the interaction between the flame and the water mist. Starting at the 500 mm position, the water mist droplets began to be entrained by the fire. Along with the entrainment, the water mist was dragging more ambient air downward. These two interactions cooled down the fire and lowered the overall flame height. With a smaller flame during water mist activation, the radiation generated by the fire also decreased.

Both the $+5^\circ$ and the -5° line of sight measurements have a similar behavior in Figure 19. They both are about 46-49% attenuation similar to the straight line of sight, then rises to 65-68% at 300 mm, 71-76% at 500 mm, and then rise again to about 82-92%. The larger attenuation values at $\pm 5^\circ$ at 300 mm below the nozzle compared to the straight line of sight might be caused by the optimum volumetric water concentration and droplet size combination like in the radiant panel results. Due to the water mist interaction with the flame, the attenuation continues to increase as 500 mm and 700 mm below the nozzle. Even though it is assumed that the droplet size is larger at 700 mm than at 500 mm and that they both are contained in the uniform turbulent region, the attenuation increases between these two points instead of decreasing like the radiant panel results. Assuming that the droplet velocity at 500 mm is a uniform 8.38 m/s [34] and the spray size is 0.005 m^2 , the concentration of water is approximately 0.166 kg/m^3 . The same assumptions are made at 700 mm, but the velocity has dropped to 4.6 m/s [34]. The new volumetric concentration is 0.3 kg/m^3 . It has been explained

above that longer residency time and higher water concentrations are better at attenuating radiation; therefore explaining why the attenuation levels increased from 500 to 700 mm below the nozzle instead of decreasing.

Overall, the attenuation levels from the diffusion flame are larger compared to the radiant panel results. One major reason why there is a difference between the two sets of results is the emitted radiation from the two heat sources. The radiant panel emits a very small range of wavelengths while the diffusion flame has a much broader range. This fuller spectrum of wavelengths gets absorbed by more of the droplets of various sizes dispersed throughout the spray. Another reason could be due to the entrainment of the water mist into the diffusion flame as it shifts back and forth.

6.4 General Remarks

When looking at the data from the two radiant heat sources, the reader will notice that there is no angular scattering data for 25, 50, and 100 mm below the nozzle. There are no data points for these locations because the horizontal crossbar supporting the water mist piping blocked the view of the heat flux gauge at the + 5° position.

It is interesting to see in Figure 20 that from the tip of the nozzle until 500 mm below, the volumetric concentration and the straight line of sight attenuation curves for both radiant heat sources have roughly the same shape. As the concentration decreases, the attenuation decreases and vice versa. This suggests that the volumetric concentration may play a larger role in the amount of attenuation than the droplet size towards the top of the spray. Once the droplet diameter exceeds a magnitude of the incident wavelength size (between 500 – 700 mm), the attenuation becomes influenced more heavily by the droplet size and decreasing even though the concentration increases.

7. Conclusion

The work presented above is the first experimental investigation of the radiation attenuation behavior through a high pressure, low flow water mist curtain. Two radiant heat sources have been used during this study; both of which produce similar trends in regards to attenuation levels at various vertical locations in the spray.

Attenuation is strongest towards the top of the spray where the droplets are smaller and the volumetric concentration of water is high. As the droplets increase in size the attenuation drops and reaches a minimum value of 42% for the radiant panel, and 57% for the diffusion flame line burner around 300 mm below the nozzle. At a point between 150 and 500 mm below the nozzle the droplet size increases and becomes more effective as its size becomes an order of magnitude off from the incident wavelength length [20] and the concentration of water begins to rise; resulting in an increased attenuation. At the 500 mm position the attenuation reached a maximum of 62% for the radiant panel and 96% for the diffusion flame line burner. It is important to note that at 500 mm below the nozzle with the diffusion flame line burner, the water mist began to interact with the flame and decreasing the flame in size. If there was no interaction between the two, it is the author's opinion that the attenuation levels would be more around 65-75%. To prevent the interaction between the water mist curtain and the fire, the author suggests that the fire size increase to 70-100+ kW; this increase in fire size would allow for a greater separation distance between the water mist curtain and the fire.

When comparing the measured attenuation levels from the radiant panel and the diffusion flame line burner, the line burner produced higher values. Due to the larger spectrum of wavelengths generated by the diffusion flame and the distribution of water droplet sizes in the curtain, more of the radiation waves are able to be absorbed and scattered. What this means is that experimental results from radiant panels and small spectrum wavelength lasers are underestimating the effectiveness of the water mist curtains when it comes to blocking radiation. On the other hand, the radiant panel results are more conservative and might be able to ensure a larger safety factor when designing a system.

The scattering of radiation away from the normal at $\pm 5^\circ$ in the vertical plane did not provide any significant findings. The complexity of the inter-scattering of radiation within the curtain is still an unknown phenomenon that could later explain their trends.

This research does support the logic that there are three key characteristics of a spray that determine the attenuation effectiveness: droplet size, volumetric water concentration, and residency time of the droplets.

Due to the time constraint to complete this project and limited fuel supply, the experiments present were not able to be run multiple times. The results given here are meant to be used as a possible trend/pilot study for future works that could investigate larger fires and multiple nozzles.

It is the author's opinion that water mist curtains can be an effective means of protecting high value targets in a calm environment. Outdoor applications may not be suitable for low flow systems because of the influence from crosswinds disrupting the curtain, considering the droplets' low inertia. Each water mist system is unique in regards to how it is characterized: operating pressure, flow rate, droplet size, etc. Just as water mist systems used out in the field need to be certified for their specific application, the research on attenuation through a water mist curtain also needs to be conducted for all combinations of pressure, flow rate, nozzle type, and droplet size.

8. Future Work

Considering how little academic research on water mist curtains as radiation shields has been completed, there are several topics that could be investigated with future work:

- Investigate the influence of environmental conditions on the spray and attenuation by a cross wind
- Place multiple micro nozzles inline between the heat source and the target both laterally and depth wise
- Use larger heat release rate diffusion fires to allow a greater distance between the heat source and the target to ensure minimal flame/water mist interactions
- Change the orientation of the nozzle from vertical to horizontal
- Change the nozzle flow rate while keeping the same pressure of 100 bar
- Perform a sensitivity analysis on the heat flux gauges used to measure the radiation. Since the measured radiant levels are so low, using heat flux gauges with a maximum range of 5 – 10 kW/m² might provide more accurate attenuation levels.

9. Acknowledgements

The author would like to thank several people for their guidance and assistance throughout this entire master's program. Firstly, Professor Bart Merci of Ghent University for organizing this program. Professor Patrick van Hees for his support here at Lund University. Associate Professor Bjarne Husted for his guidance, supervision, and insight throughout the entire thesis process. Associate Professor Stefan Svensson for his assistance with the experiments and equipment setup. Danfoss for their generous donation of the water mist pump and Danfoss-Semco for the nozzles, piping, and hoses. Jasper Ho for his support and extra set of hands during the entire thesis. Lastly, the Illinois Fire Service Institute Library for their assistance in finding Fire Service specific articles on water mist.

10. References

1. Spadafora, Ronald. "Halon Replacement: Water Mist Fire Extinguishing Systems." *Fire Engineering* January 2008.
2. Husted, Bjarne P. *Experimental measurements of water mist systems and implications for modelling in CFD*. PhD Thesis. Lund: Department of Fire Safety Engineering, Lund University, 2007.
3. Mawhinney, J R and G G Back III. "Section 4: Chapter 14: Water Mist Fire Suppression Systems." *SFPE Handbook of Fire Protection Engineering*. Quincy, Massachusetts: NFPA, 2002.
4. Shiner, Andrew. "Clearing the Fog Around Water Mist." *Fire Safety Systems* Dec 2007-Jan 2008: 20.
5. Leeds, Stephen. "Water-Mist Fire Suppression Systems." *Fire Engineering* June 1994: 66-68.
6. Mawhinney, J R. "Water Mist Suppression Systems May Solve an Array of Fire Protection Problems." *NFPA Journal* May/June 1994: 46-57.
7. Ruland, Scott and Tyler Aebersold. "Effective Water Mist System Design Lessens Fire Danger." *Power Engineering* December 1999: 200-204.
8. Annable, Kelvin. "Water Mist Systems for Prison Cells." *Fire Safety Systems* Dec 2009-Jan 2010: 12-14.
9. Horton, Glenn and David Yirrell. "Out of the Mist." *Fire Safety Systems* May 2006: 32-34.
10. Adiga, K C. "Ultrafine Water Mist Fire Suppression Technology." *Fire Engineering* January 2005: 197-200.
11. Lefebvre, Arthur H. *Atomization and Sprays*. Boca Raton, FL: Taylor & Francis Group, LLC, 1989.
12. Murrell, J V, D Crowhurst and P Rock. "Experimental Study of the Thermal Radiation Attenuation of Sprays from Selected Hydraulic Nozzles." *Halon Options Technical Working Conference 1995*. Albuquerque, 1995. 369-378.
13. Dembele, S, A Delmas and J F Sacadura. "A Method for Modeling the Mitigation of Hazardous Fire Thermal Radiation by Water Spray Curtains." *Journal of Heat Transfer* 119 (1997): 746-753.
14. Dembele, S, J X Wen and J F Sacadura. "Experimental Study of Water Sprays for the Attenuation of Fire Thermal Radiation." *Journal of Heat Transfer* (June 2001): 534-543.

15. Boulet, P, A Collin and G Parent. "Heat transfer through a water spray curtain under the effect of a strong radiative source." *Fire Safety Journal* 41 (2006): 15-30.
16. Collin, A, et al. "On radiative transfer in water spray curtains using the discrete ordinates method." *Journal of Quantitative Spectroscopy & Radiative Transfer* 92 (2005): 85-110.
17. Mawhinney, J R, B Z Dlugogorski and A K Kim. "A Closer Look at the Fire Extinguishing Properties of Water Mist." *Fire Safety Science-Proceedings of the Fourth International Symposium*. International Association of Fire Safety Science, 1994. 47-60.
18. Ravigururajan, T S and M R Beltran. "A Model for Attenuation of Fire Radiation Through Water Droplets." *Fire Safety Journal* 15 (1989): 171-181.
19. Berour, N, et al. "Radiative and conductive heat transfer in a nongrey semitransparent medium. Application to fire protection curtains." *Journal of Quantitative Spectroscopy & Radiative Transfer* 86 (2004): 9-30.
20. Coppalle, A. "Fire Protection: Water Curtains." *Fire Safety Journal* 20 (1993): 241-255.
21. Dubay, Christian. "The Effects of Water Mist on Interior Firefighting." *Fire Engineering* November 1996: 78-79.
22. Hostikka, Simo and K McGrattan. "Numerical modeling of radiative heat transfer in water sprays." *Fire Safety Journal* 41 (2006): 76-86.
23. Collin, A, et al. "Dynamics of thermal behaviour of water sprays." *International Journal of Thermal Science* 47 (2008): 399-407.
24. Collin, A, et al. "Water Mist and Radiation Interactions: Application to a Water Curtain Used as a Radiative Shield." *Numerical Heat Transfer; Part A: Applications* 57 (2010): 537-553.
25. Thomas, P H. "Absorption and scattering of radiation by water sprays of large drops." *British Journal of Applied Physics* 3 (1952): 385-393.
26. Viskanta, R and C C Tseng. "Spectral radiation characteristics of water sprays." *Combustion Theory and Modeling* 11.1 (2007): 113-125.
27. Yang, Wenhua, et al. "The interaction of thermal radiation and water mist in fire suppression." *Fire Safety Journal* 39 (2004): 41-66.
28. Reischl, Uwe. "Water Fog Stream Heat Radiation Attenuation." *Fire Technology* (1979): 262-270.
29. Heselden, A J M and P L Hinkley. "Measurements of the Transmission of Radiation Through Water Sprays." *Fire Technology* (1965).

30. Parent, G, et al. "Experimental Investigation of Radiation Transmission Through a Water Spray." *Journal of Quantitative Spectroscopy & Radiative Transfer* (2006): 126-141.
31. Drysdale, Dougal. *An Introduction to Fire Dynamics*. 3rd. West Sussex: John Wiley & Sons, Ltd., Publications, 2011.
32. Karlsson, B and J Quintiere. *Enclosure Fire Dynamics*. Boca Raton: CRC Press LLC, 2000.
33. Husted, Bjarne, G Holmstedt and T Hertzberg. "The physics behind water mist systems." *Proceedings of the International Water Mist Association Conference*. Rome, Italy, 2004.
34. Husted, Bjarne, et al. "Comparison of PIV and PDA droplet velocity measurement techniques on two high-pressure water mist nozzles." *Fire Safety Journal* (2009): 1030-1045.
35. Laven, P. "MiePlot - Computer program for scattering of light from a sphere using Mie theory & the Debye series." Geneva, Switzerland, 2005.
36. Försth, Michael and Kenneth Möller. "Absorption of heat radiation in liquid droplets." 2011.
37. Sunahara, Hiroyuki and et. al. "A study on relation between heat release rate and radiative heat flux of wood cribs burning during water discharge." *Journal of Environmental Engineering* 75 (2010): 1009-1017.
38. Danfoss. "Technical Data Sheet-Water Mist Nozzles." May 2011. 15 March 2015. <http://www.danfoss.com/NR/rdonlyres/CB7DD9DF-9AD2-476F-A2C3-5E5B6ABECA96/0/521B0563_DKCFNPD091A702_WaterMistNozzles_GB.pdf>.

Appendix A: Photographs



Figure A-1 . Danfoss Power Pack PPH 6.3 with a piston pump used throughout the study



Figure A-2 . Propane radiant panel 0.39 x 0.47 m



Figure A-3 . Line gas burner 0.02 x 0.39 m

Appendix B: Flow Rate Test Procedure

To test the flow rate stated in the Danfoss specifications sheet, the following procedure was used. First a bucket and a plastic bag were weighed to get baseline weight data. The plastic bag was placed over the nozzle to capture and direct all the fine water particles into the bucket. The water mist system was turned on for 5 minutes. After 5 minutes the water, bucket, and plastic bag were weighed again. The final total weight was subtracted by the initial bucket and bag weight. This new weight was converted from kg to L, and divided by the testing time (5 min). This resulted in a value of 0.418 L/min at 100 bar operating pressure. This was equivalent to the data in Table B-1.

Table B-1. Danfoss 1910 specification [38].

Litre per hour	Litre per min.	US Gallon per hour	US Gallon per min.	Spray angle	Operating pressure / Max. pressure bar (psi)	Nozzle / hose Material	Nozzle thread	Code number
25.2	0.42	6.6	0.1	60°	100 / 130 (1450 / 1900)	AISI316 / 430	M13 × 1 mm	180Z1910

Appendix C: Heat Flux Gauge Calibration

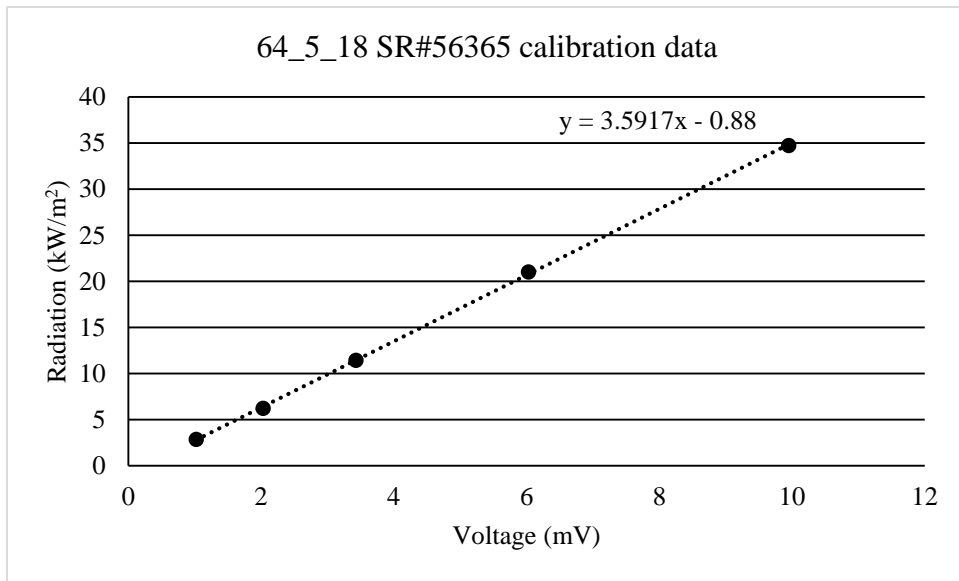


Figure C-1. MedTherm 64-5-18 calibration curve

Appendix D: Experimental Procedure

1. Motivation

The following document outlines the experimental tests that will be conducted in order to complete my IMFSE thesis: The use of a water mist curtain as a radiation shield. Water mist systems have become more popular over the years as an effective alternative to many outlawed Halon suppression systems and for shipboard fire containment. Besides suppressing the fire, water mist systems have started being considered as a means of protecting high value areas within a structure by controlling flame spread by forming a shield between the fire and the target. This application has been proposed based on the mist's ability to reduce/scatter/absorb the electromagnetic radiation waves being transported from the fire source onto a target on the other side of the curtain. These tests will provide some of the first experimental data on radiation attenuation through water mist at high pressures from various gas powered heat sources.

2. Experimental Set-up

This section describes the test setup used in the fire lab for my IMFSE thesis. There are two different heat source configurations that will be used: propane fueled radiant panel and a gas diffusion line burner with propane. For all tests and configurations, the same mist nozzle will be used: a Danfoss 1910 micro nozzle with an output of 0.42 L/min at 100 bar. The nozzle itself is attached to an aluminum superstructure that can move up and down independently from the heat source and heat flux gauge. For the radiant panel experiments, the following setup will be used (Figure 1). The panel is 39 cm wide and 47 cm tall. Radiation will be measured with and without the sprinkler to establish the attenuation. The heat flux gauge will be placed directly in front of the panel and positioned to face the center of the panel.

Radiant panel

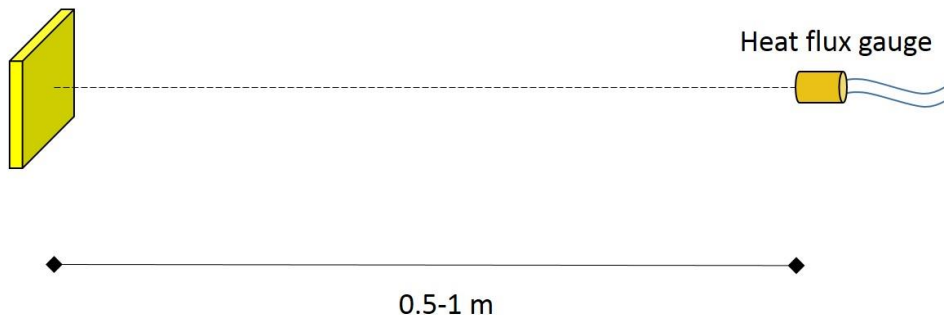


Figure 1. Radiant panel baseline setup

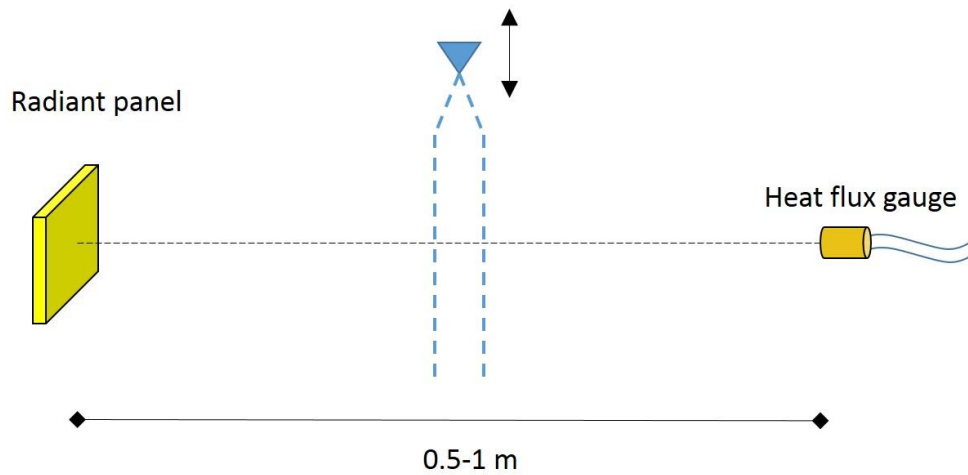


Figure 2. Radiant panel sprinkler setup (drawing not to scale).

The sprinkler head will be moved up and down to see the attenuation based on the vertical position within the mist column (from the cone to the turbulent region)(Figure 2). As seen in Figure 3, the angle of the heat flux gauge will be changed to measure the scattering of the radiation from the normal.

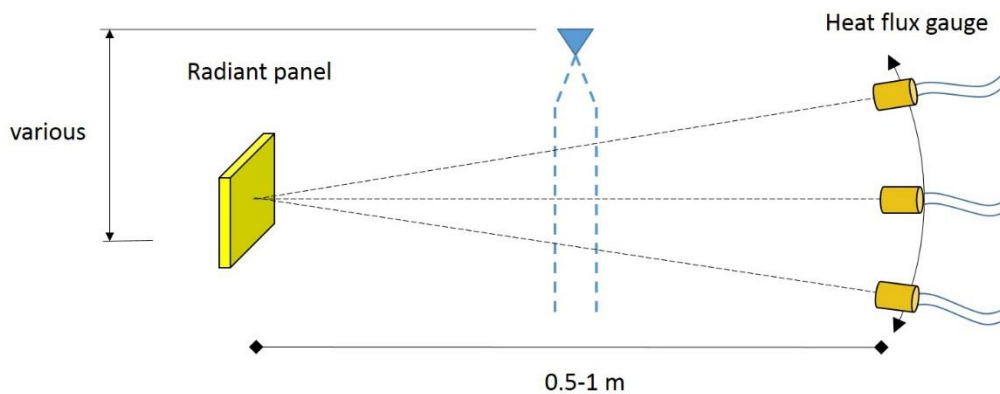


Figure 3. Manipulation of the angle of the heat flux gauge in relation to the horizontal (drawing not to scale).

For the second heat source (gas line burner), a similar set up will be used (Figure 4). The burner area is about 2 cm x 39 cm. First the vertical position within the flame/plume region with the highest radiant heat flux needs to be established. The gas flow rate will be set and measured by a flow meter to calculate a constant HRR of the fire no matter the fuel.

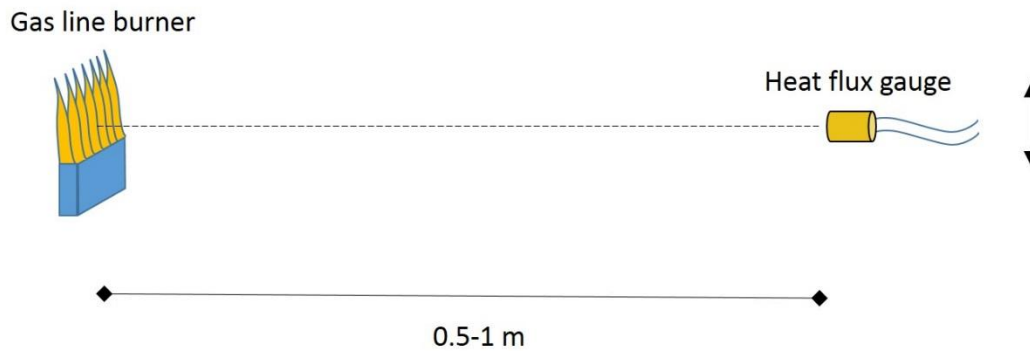


Figure 4. Initial heat flux measurement determination without sprinkler (drawing not to scale).

Once the height of the heat flux gauge is set, the initial heat flux is measured without the water mist. Next the mist is turned on and the nozzle is moved vertically to measure the attenuation based on the vertical position within the mist (Figure Figure 5): cone, transition region, and turbulent steady state region.

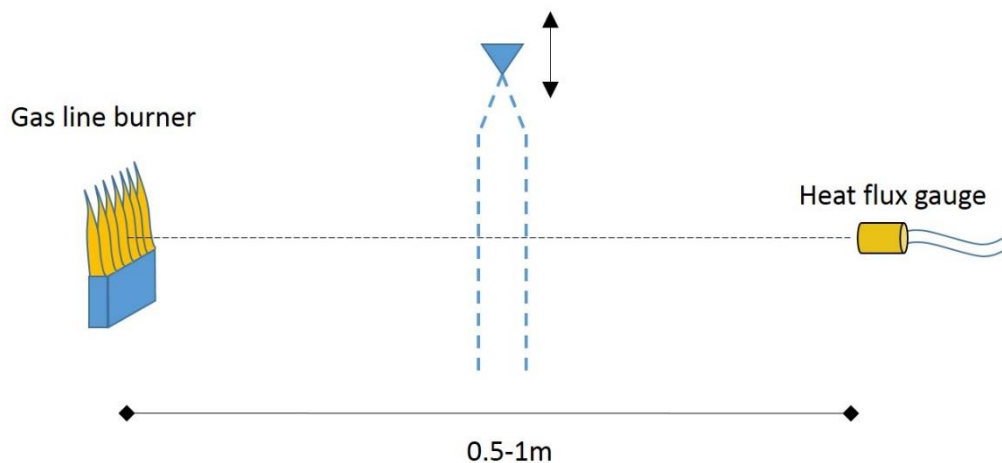


Figure 5. Gas line burner set up with adjustable sprinkler height (drawing not to scale).

Lastly, the heat flux gauge will be adjusted to look at the flame from various angles to investigate the forward scattering. The heat flux gauge will stay in plane and “rotate” around the flame vertically as if the fire was the center of a circle (Figure 6).

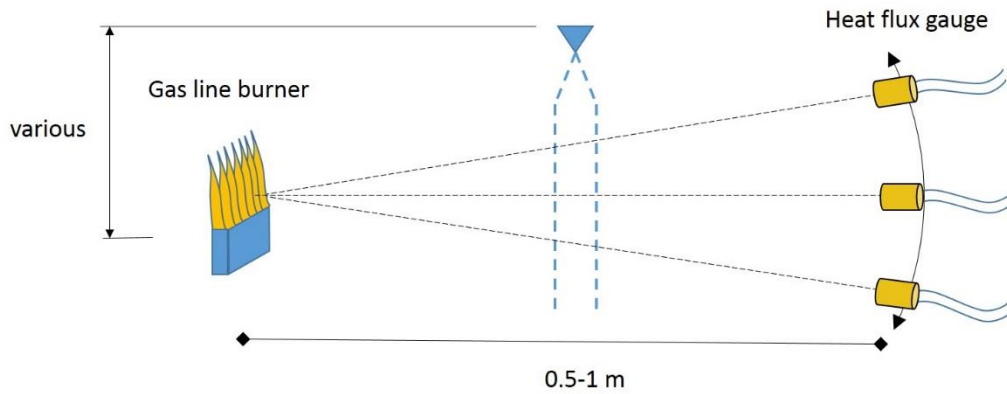


Figure 6. Manipulation of the angle of the heat flux gauge in relation to the horizontal (drawing not to scale).

Propane gas was used to create the necessary heat flux. The distance between the flame and the heat flux gauge will be set between 0.5 - 1 m.

To generate the 100 bar pressure needed to feed the nozzle, a high pressure water pump unit was used. The high pressure pump being used is a Danfoss power pack PPH 6.3 piston pump. This pump sits on top of the water reservoir that recirculates its excess water. The reservoir is continuously filled with cool water with a runoff line to ensure that the reservoir water stays at a consistent temperature. If the temperature of the supplied water to the nozzle were to rise over time, the characteristics of the water would be different with time (viscosity, temperature, evaporation time, specific heat, etc.)

3. Measurement Set-up

The following measurement devices will be used for this experiment. A gas flow meter will measure the amount of gas being provided to the burner in L/min. A high pressure gauge will be placed near the nozzle to ensure that the nozzle pressure is $100 \text{ bar} \pm 2$. One or multiple heat flux gauges will be used to measure the radiant heat flux from the radiant panel or the gas line burner (Medtherm model 64-05-18). It is the author's understanding that the heat flux gauge used is a Gardon type gauge. This means that the convective heat transfer at the surface of the device is not taken into account; therefore, only receiving the radiative flux from the heat source. The initial position of the heat flux gauge will be determined by iterations based on the maximum heat flux received by the fire without the water mist. For the radiant panel, the heat flux gauge will be directed towards the center of the panel; both vertically and horizontally. A thermocouple will be placed in the water reservoir to ensure constant temperature of the supply water.

4. Step-By-Step Procedure

4.1 Radiant panel heat source

2. Put on protective equipment
3. Place experimental procedure and risk assessment on the door
4. Turn on ventilation
5. Setup equipment (measurement, burners, etc)
6. Turn on the data acquisition
7. Turn on cooling water for the heat flux gauge
8. Calibrate equipment
9. Turn on gas and check for leaks
10. Ignite radiant panel, set to desired temperature and let stabilize, and note the flow rate
11. Measure the baseline radiant heat flux at the center of the panel
12. Turn on the water mist, and measure the new heat flux
13. Change the vertical position of the nozzle head (cone, transition region, steady state turbulent region) and measure the heat flux
14. Change the angle of the heat flux gauge while keeping it pointed at the same location of the flame
15. Stop data collection and dump data
16. Repeat steps 4-14, changing the temperature of the radiant panel and repeat as many times as needed (best to start at lower temperatures and work upward)
17. Turn off the gas
18. Turn off all water supplies
19. Remove the test equipment and clean up the lab
20. Transfer all data off the computer to a USB device
21. Ensure everything is in initial conditions
22. Shut down ventilation
23. Leave the lab and ensure it's locked up
24. Give the key to the supervisor
25. Remove experimental procedure and risk assessment from the door
26. Return protective equipment

4.2 Gas line burner heat source

1. Put on protective equipment
2. Place experimental procedure and risk assessment on the door
3. Turn on ventilation

4. Setup equipment (measurement, burners, etc)
5. Turn on the data acquisition
6. Turn on cooling water for the heat flux gauge
7. Calibrate equipment
8. Turn on gas and check for leaks
9. Ignite burner
10. Set mass flow rate to reach a HRR of ##(##L/min)
11. Measure the radiant heat flux until the vertical position is found for the max value
12. Measure the baseline radiant heat flux without the mist
13. Turn on the water mist system and let stabilize to 100 bar, and measure the new heat flux
14. Change the vertical position of the nozzle head (cone, transition region, steady state turbulent region) and measure the heat flux
15. Change the angle of the heat flux gauge while keeping it pointed at the same location in the flame
16. Turn off the gas
17. Turn off water pump
18. Stop data collection and dump data
19. Repeat steps 4-18 with the remain fuel sources
20. Remove the test equipment and clean up the lab
21. Transfer all data off the computer to a USB device
22. Ensure everything is in initial conditions
23. Shut down ventilation
24. Leave the lab and ensure it's locked up
25. Give the key to the supervisor
26. Remove experimental procedure and risk assessment from the door
27. Return protective equipment

Appendix

Heat sources



Figure 7. Gas radiant panel



Figure 8. Gas line burner

Appendix E: Risk Assessment

Introduction

The following document is intended to be used as a risk assessment for the experiments needed to complete the master's thesis entitled "The Use of a Water Mist Curtain as a Radiation Shield".

Value and Objectives

Ensure Safety/Health of the research team and building staff.

Protect Property and Lab Equipment

Obtain accurate and consistent Results

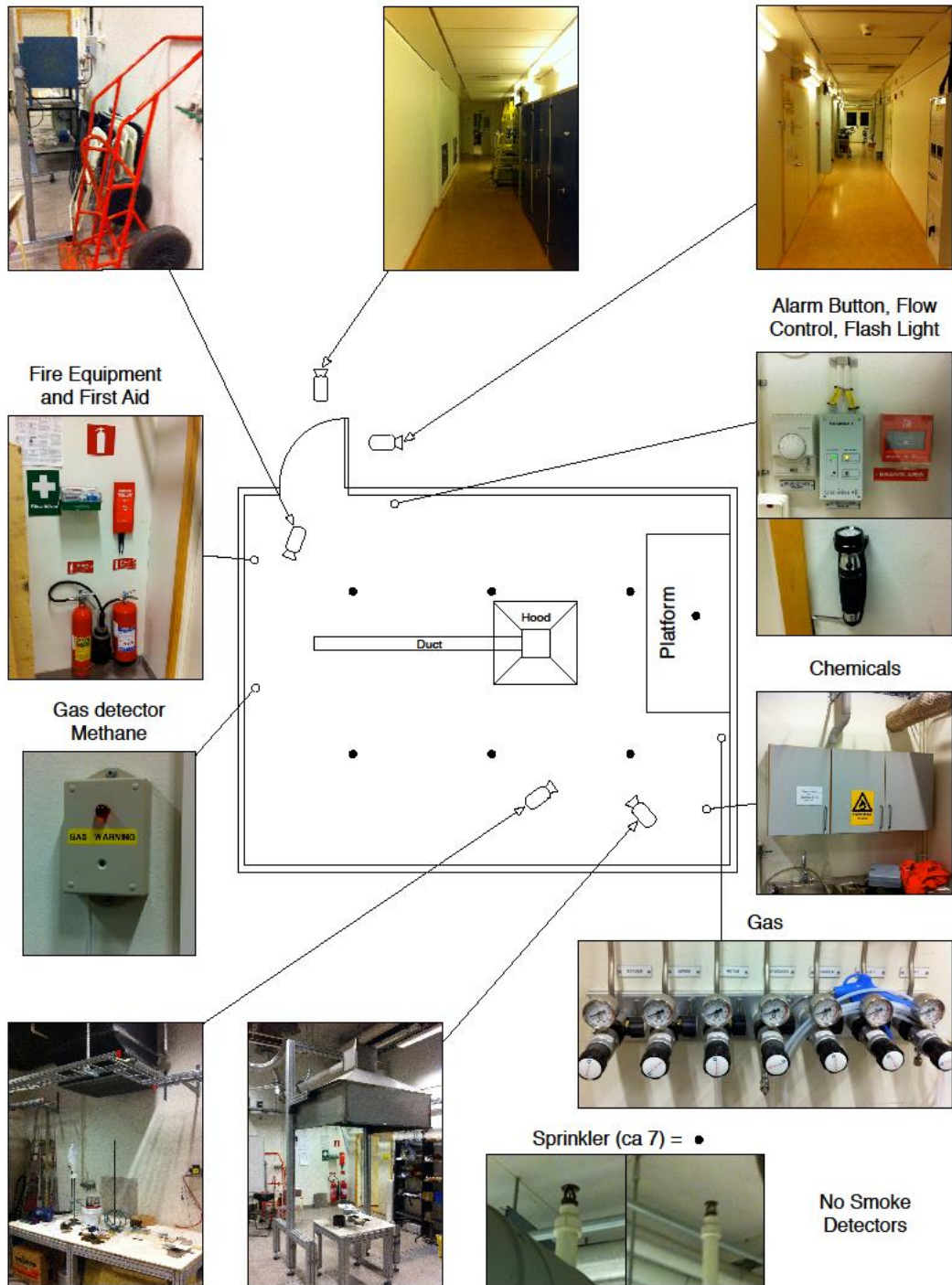
Static Model

Boundary Conditions

The following tests will be conducted in the Physics building in the E block in the fire testing lab rm. E231. Figure 1 shows a diagram of the fire lab with the various fire protection systems marked on the map.

Testing Equipment Available

- Thermocouples (K type)
- Heat Flux gauges
- Flow meters
- Video cameras
- High pressure electric water pump
- Propane radiant heat Panel
- Gas line burner



by
Daniel Nilsson
2014-01-20

Figure 1. Boundary conditions and safety features within the fire laboratory in the Physics building.

Dynamic Model

Dynamic Model Radiant Panel

1. Put on protective equipment
2. Place experimental procedure and risk assessment on the door
3. Turn on ventilation
4. Setup equipment (measurement, burners, etc.)
5. Turn on the data acquisition
6. Turn on cooling water for the heat flux gauge
7. Calibrate equipment
8. Turn on gas and check for leaks
9. Ignite radiant panel, set to desired temperature and let stabilize, and note the flow rate
10. Measure the baseline radiant heat flux at the center of the panel
11. Turn on the water mist, and measure the new heat flux
12. Change the vertical position of the nozzle head (cone, transition region, steady state turbulent region) and measure the heat flux
13. Change the angle of the heat flux gauge while keeping it pointed at the same location of the flame
14. Stop data collection and dump data
15. Repeat steps 4-14, changing the temperature of the radiant panel and repeat as many times as needed (best to start at lower temperatures and work upward)
16. Turn off the gas
17. Turn off all water supplies
18. Remove the test equipment and clean up the lab
19. Transfer all data off the computer to a USB device
20. Ensure everything is in initial conditions
21. Shut down ventilation
22. Leave the lab and ensure it's locked up
23. Give the key to the supervisor
24. Remove experimental procedure and risk assessment from the door
25. Return protective equipment

Dynamic Model Gas Line Burner

1. Put on protective equipment
2. Place experimental procedure and risk assessment on the door

3. Turn on ventilation
4. Setup equipment (measurement, burners, etc.)
5. Turn on the data acquisition
6. Turn on cooling water for the heat flux gauge
7. Calibrate equipment
8. Turn on gas and check for leaks
9. Ignite burner
10. Set mass flow rate to reach a HRR of ##(##L/min)
11. Measure the radiant heat flux until the vertical position is found for the max value
12. Measure the baseline radiant heat flux without the mist
13. Turn on the water mist system and let stabilize to 100 bar, and measure the new heat flux
14. Change the vertical position of the nozzle head (cone, transition region, steady state turbulent region) and measure the heat flux
15. Change the angle of the heat flux gauge while keeping it pointed at the same location in the flame
16. Turn off the gas
17. Turn off water pump
18. Stop data collection and dump data
19. Repeat steps 4-18 with the remain fuel sources
20. Remove the test equipment and clean up the lab
21. Transfer all data off the computer to a USB device
22. Ensure everything is in initial conditions
23. Shut down ventilation
24. Leave the lab and ensure it's locked up
25. Give the key to the supervisor
26. Remove experimental procedure and risk assessment from the door
27. Return protective equipment

What If Analysis

Assumptions: only values/objectives that could be affected are addressed

Radiant Panel Assessment

	Event	Causes	Consequences	Present protection	Preventive measures
1	<i>Check if the building/lab is unlocked</i>				
	Results	Door is locked to the lab/building	Not able to run the experiment	knock on the door	Have contact information for lab manager/professor for assistance
2	<i>Put on protective gear</i>				
	safety/health	protective gear not available	Personal injury	more protective gear available compared to the number of students	Have contact information for lab manager/professor for assistance
	results	cannot enter lab	Not able to run the experiment	more protective gear available compared to the number of students	Have contact information for lab manager/professor for assistance
3	<i>Place experimental procedure and risk analysis sheets on the door</i>				
	safety/health	team forgot the documentation	potential injury to the team and other occupants in the building	documentation must be present and approved	each team member has a copy
	Property and Equipment	team forgot the documentation	will not be able to use the facilities	documentation must be present and approved	each team member has a copy
	Results	team forgot the documentation	will not be able to run the experiments	documentation must be present and approved	each team member has a copy

4	<i>Check/Start Ventilation</i>				
	safety/health	ventilation it's not working	possible risk of personal injury in case of uncontrolled experiment	check that ventilation is working at the present moment	Have contact information for lab manager/professor for assistance
	Property and Equipment	ventilation it's not working	possible damage to equipment and the building due to smoke and heat	check that ventilation is working at the present moment	Have contact information for lab manager/professor for assistance
	Results	ventilation it's not working	Not able to run the experiment	check that ventilation is working at the present moment	Have contact information for lab manager/professor for assistance
5	<i>Ensure safety detection systems are in place/operational</i>				
	safety/health	they are not in proper conditions	possible risk for human safety in case of uncontrolled experiment	check that they are working at the present moment	Have contact information for lab manager/professor for assistance
	Property and Equipment	they are not in proper conditions	possible risk for property in case of uncontrolled experiment	check that they are working at the present moment	Have contact information for lab manager/professor for assistance
	Results	they are not in proper conditions	Not able to run the experiment	check that they are working at the present moment	Have contact information for lab manager/professor for assistance
6	<i>Turn on/Calibrate/check for appropriate data transfer of the test equipment</i>				
	Property and Equipment	Improper calibration	Damage to testing equipment	Calibration training with the lab manager	Follow the same procedure as the calibration lab session
	Results	something is not working	Not able to run the experiment	check that they are working at the present moment	Have contact information for lab manager/professor for assistance

7	<i>Setup experimental equipment</i>				
	safety/health	something breaks	possible injuries	ensure everyone knows how to operate the equipment	conduct equipment training
	Property and Equipment	something breaks	loss of needed material	ensure everyone knows how to operate the equipment	conduct equipment training
	Results	something breaks	Not able to run the experiment	ensure everyone knows how to operate the equipment	conduct equipment training
8	<i>Check water supply</i>				
	Property and Equipment	Blockage, lack of water, forgot to turn it on	damage to equipment	none	double check water supply
	Results	Blockage, lack of water, forgot to turn it on	unable to gain accurate results	none	double check water supply
9	<i>Connect fuel source to the radiant panel</i>				
	safety/health	there are leaks at the connections	possible risk for human heath/possible explosion	check that there are no leaks at the present moment	conduct training on fuel sources and methods of connecting
	Property and Equipment	there are leaks at the connections	possible risk for damaged equipment/explosion	check that there are no leaks at the present moment	conduct training on fuel sources and methods of connecting
	Results	there are leaks at the connections	Not able to run the experiment	check that there are no leaks at the present moment	conduct training on fuel sources and methods of connecting

10	<i>Check for fuel leaks at the connections</i>				
	safety/health	there are leaks at the connections	possible risk for human heath/possible explosion	check that there are no leaks at the present moment	conduct training on fuel sources and methods of connecting
	Property and Equipment	there are leaks at the connections	possible risk for damaged equipment/explosion	check that there are no leaks at the present moment	conduct training on fuel sources and methods of connecting
	Results	there are leaks at the connections	Not able to run the experiment	check that there are no leaks at the present moment	conduct training on fuel sources and methods of connecting
11	<i>Ignite radiant panel</i>				
	safety/health	ignites suddenly	possible injuries	learn proper setup and ignition procedure	ensure it's turned off before installation
	Property and Equipment	ignites suddenly	destruction of equipment/building	learn proper setup and ignition procedure	ensure it's turned off before installation
	Results	ignites suddenly	Not able to run the experiment	learn proper setup and ignition procedure	ensure it's turned off before installation
12	<i>Set flow rate/desired temperature and document</i>				
	Property and Equipment	Equipment does not work properly	Not able to measure mass flow rate	Calibration before lab	calibration after each experiment
	Results	Equipment does not work properly	Not able to measure mass flow rate	Calibration before lab	calibration after each experiment

13	<i>Experimental procedure</i>				
	safety/health	part of the procedure is dangerous for people (gases, high temp)	someone might get injured	risk analysis	risk analysis, ensure each team member knows their task
	Property and Equipment	Due to experiment conditions, equipment might be damage	Cannot continue with the lab.	procedure will be checked by lab supervisor	Ensure equipment is suitable for the lab conditions (temp, time, etc.)
	Results	not following each step properly	no data collected	review the procedure before conducting the experiments	follow the procedure during the experiments
14	<i>Save data and export</i>				
	Property and Equipment	Equipment might be damage	can't get data	Calibrations	take some data before experiments in order to check the equipment
	Results	Equipment might be damage	no results for conclusions	Calibrations	take some data before experiments in order to check the equipment
15	<i>Repeat steps 7-14 based on number of experimental iterations</i>				
16	<i>Shut down gas supply</i>				
	safety/health	gas supply not shut down properly	someone might get burned, or breath harmful gases	follow procedure for cooling down equipment	double check that the valve is turned off at the supply
	Property and Equipment	gas supply not shut down properly	damage to the heat source/building	follow procedure for disassembly of equipment	double check that the valve is turned off at the supply
17	<i>Transfer test data to backups</i>				
	Results	Malfunctioning Data Acquisition	Data unable to be transferred	Online backup with the DAQ system	Backup data after every experiment

18	<i>Shutdown equipment</i>				
	Property and Equipment	Improper shut down procedure	Damage to testing equipment	Lab equipment training for students	Lab manager present during testing
19	<i>Clean up lab/return to starting conditions</i>				
	safety/health	Slip/trip/falls, and not wearing proper protective equipment	Personal Injury	wearing protective equipment provided	work slowly and with a purpose
20	<i>Shut down ventilation</i>				
	Property and Equipment	ventilation system not shut down	Other lab experiments might be affected by the change in air flow	Lab manager present to assist with lab protocol	Place this step in the experimental procedure
21	<i>Lock up/leave lab with supervisor</i>				
	Property and Equipment	Equipment stolen/broken	University must pay to replace or pay for repairs	Lab manager present to assist with lab protocol	Place this step in the experimental procedure
22	<i>Remove experimental procedure and risk assessment from the door</i>				
23	<i>Remove/put away protective equipment</i>				
	safety/health	Slip/trip/falls	personal injury	none	take off protective gear slowly and while seated

Gas Line Burner Assessment

	Event	Causes	Consequences	Present protection	Preventive measures
1	<i>Check if the building/lab is unlocked</i>				
	Results	Door is locked to the lab/building	Not able to run the experiment	knock on the door	Have contact information for lab manager/professor for assistance
2	<i>Put on protective gear</i>				
	safety/health	protective gear not available	Personal injury	more protective gear available compared to the number of students	Have contact information for lab manager/professor for assistance
	results	cannot enter lab	Not able to run the experiment	more protective gear available compared to the number of students	Have contact information for lab manager/professor for assistance
3	<i>Place experimental procedure and risk analysis sheets on the door</i>				
	safety/health	team forgot the documentation	potential injury to the team and other occupants in the building	documentation must be present and approved	each team member has a copy
	Property and Equipment	team forgot the documentation	will not be able to use the facilities	documentation must be present and approved	each team member has a copy
	Results	team forgot the documentation	will not be able to run the experiments	documentation must be present and approved	each team member has a copy

4	<i>Check/Start Ventilation</i>				
	safety/health	ventilation it's not working	possible risk of personal injury in case of uncontrolled experiment	check that ventilation is working at the present moment	Have contact information for lab manager/professor for assistance
	Property and Equipment	ventilation it's not working	possible damage to equipment and the building due to smoke and heat	check that ventilation is working at the present moment	Have contact information for lab manager/professor for assistance
	Results	ventilation it's not working	Not able to run the experiment	check that ventilation is working at the present moment	Have contact information for lab manager/professor for assistance
5	<i>Ensure safety detection systems are in place/operational</i>				
	safety/health	they are not in proper conditions	possible risk for human safety in case of uncontrolled experiment	check that they are working at the present moment	Have contact information for lab manager/professor for assistance
	Property and Equipment	they are not in proper conditions	possible risk for property in case of uncontrolled experiment	check that they are working at the present moment	Have contact information for lab manager/professor for assistance
	Results	they are not in proper conditions	Not able to run the experiment	check that they are working at the present moment	Have contact information for lab manager/professor for assistance
6	<i>Turn on/Calibrate/check for appropriate data transfer of the test equipment</i>				
	Property and Equipment	Improper calibration	Damage to testing equipment	Calibration training with the lab manager	Follow the same procedure as the calibration lab session
	Results	something is not working	Not able to run the experiment	check that they are working at the present moment	Have contact information for lab manager/professor for assistance

7	<i>Setup experimental equipment</i>				
	safety/health	something breaks	possible injuries	ensure everyone knows how to operate the equipment	conduct equipment training
	Property and Equipment	something breaks	loss of needed material	ensure everyone knows how to operate the equipment	conduct equipment training
8	Results	something breaks	Not able to run the experiment	ensure everyone knows how to operate the equipment	conduct equipment training
	<i>Check water supply</i>				
	Property and Equipment	Blockage, lack of water, forgot to turn it on	damage to equipment	none	double check water supply
9	Results	Blockage, lack of water, forgot to turn it on	unable to gain accurate results	none	double check water supply
	<i>Connect fuel source to the burner</i>				
	safety/health	there are leaks at the connections	possible risk for human heath/possible explosion	check that there are no leaks at the present moment	conduct training on fuel sources and methods of connecting
9	Property and Equipment	there are leaks at the connections	possible risk for damaged equipment/explosion	check that there are no leaks at the present moment	conduct training on fuel sources and methods of connecting
	Results	there are leaks at the connections	Not able to run the experiment	check that there are no leaks at the present moment	conduct training on fuel sources and methods of connecting

10	<i>Check for fuel leaks at the connections</i>				
	safety/health	there are leaks at the connections	possible risk for human heath/possible explosion	check that there are no leaks at the present moment	conduct training on fuel sources and methods of connecting
	Property and Equipment	there are leaks at the connections	possible risk for damaged equipment/explosion	check that there are no leaks at the present moment	conduct training on fuel sources and methods of connecting
	Results	there are leaks at the connections	Not able to run the experiment	check that there are no leaks at the present moment	conduct training on fuel sources and methods of connecting
11	<i>Ignite Line Burner</i>				
	safety/health	ignites suddenly	possible injuries	learn proper setup and ignition procedure	ensure it's turned off before installation
	Property and Equipment	ignites suddenly	destruction of equipment/building	learn proper setup and ignition procedure	ensure it's turned off before installation
	Results	ignites suddenly	Not able to run the experiment	learn proper setup and ignition procedure	ensure it's turned off before installation
12	<i>Set flow rate and document</i>				
	Property and Equipment	Equipment does not work properly	Not able to measure mass flow rate	Calibration before lab	calibration after each experiment
	Results	Equipment does not work properly	Not able to measure mass flow rate	Calibration before lab	calibration after each experiment

13	<i>Experimental procedure</i>				
	safety/health	part of the procedure is dangerous for people (gases, high temp)	someone might get injured	risk analysis	risk analysis, ensure each team member knows their task
	Property and Equipment	Due to experiment conditions, equipment might be damage	Cannot continue with the lab.	procedure will be checked by lab supervisor	Ensure equipment is suitable for the lab conditions (temp, time, etc.)
	Results	not following each step properly	no data collected	review the procedure before conducting the experiments	follow the procedure during the experiments
14	<i>Save data and export</i>				
	Property and Equipment	Equipment might be damage	can't get data	Calibrations	take some data before experiments in order to check the equipment
	Results	Equipment might be damage	no results for conclusions	Calibrations	take some data before experiments in order to check the equipment
15	<i>Repeat steps 7-14 based on number of experimental iterations</i>				
16	<i>Shut down gas supply</i>				
	safety/health	gas supply not shut down properly	someone might get burned, or breath harmful gases	follow procedure for cooling down equipment	double check that the valve is turned off at the supply
	Property and Equipment	gas supply not shut down properly	damage to the heat source/building	follow procedure for disassembly of equipment	double check that the valve is turned off at the supply
17	<i>Transfer test data to backups</i>				
	Results	Malfunctioning Data Acquisition	Data unable to be transferred	Online backup with the DAQ system	Backup data after every experiment

<i>Shutdown equipment</i>					
18	Property and Equipment	Improper shut down procedure	Damage to testing equipment	Lab equipment training for students	Lab manager present during testing
<i>Clean up lab/return to starting conditions</i>					
19	safety/health	Slip/trip/falls, and not wearing proper protective equipment	Personal Injury	wearing protective equipment provided	work slowly and with a purpose
<i>Shut down ventilation</i>					
20	Property and Equipment	ventilation system not shut down	Other lab experiments might be affected by the change in air flow	Lab manager present to assist with lab protocol	Place this step in the experimental procedure
<i>Lock up/leave lab with supervisor</i>					
21	Property and Equipment	Equipment stolen/broken	University must pay to replace or pay for repairs	Lab manager present to assist with lab protocol	Place this step in the experimental procedure
22	<i>Remove experimental procedure and risk assessment from the door</i>				
<i>Remove/put away protective equipment</i>					
23	safety/health	Slip/trip/falls	personal injury	none	take off protective gear slowly and while seated